The Effects of Bisphosphonate on Direct Fracture Healing

Terence Savaridas

MD

The University of Edinburgh

2011

Abstract

Fractures repair by two distinct mechanism; indirect fracture healing via an endochondral stage and direct fracture healing with primary bone formation via osteonal remodelling units ('cutting cones'). Bisphosphonates are recommended by national clinical guidelines to reduce the risk of osteoporotic fractures. Despite bisphosphonate therapy, osteoporotic fractures continue to occur. A proportion of these fractures require rigid fixation, whereby bone repairs by direct fracture healing.

The effects of bisphosphonate therapy on direct fracture healing have not been previously reported. With indirect fracture healing, therapeutic doses of bisphosphonate led to a delay in callus remodelling and a larger callus volume without detrimental effects on the physical property of healing fractures.

A model of direct fracture healing with rigid tibial plating in the rat was developed. In addition, a non-rigid model of external fixation that used the same number and size of screw holes to that of the plating model was used for comparison. Implants were designed and tested in cadavers prior to preliminary studies in rats.

Within these two groups, animals were randomly allocated either to receive daily injections of bisphosphonate (Ibandronate) or saline (Control) for nine weeks. Following three weeks of injections a transverse tibial osteotomy was created and stabilised. Plain radiographs were obtained at fortnightly intervals. Animals were sacrificed at six weeks post fracture stabilisation. On sacrifice, fracture healing was assessed on contact radiographs, with a 4-point bend to failure and histologically. The mechanical properties of the uninjured diaphyseal bone in the contra-lateral limb were also assessed following bisphosphonate therapy.

The mean bending stress at failure of diaphyseal bone in the uninjured limb was increased by 20% following only nine weeks of bisphosphonate treatment. The increase in strength of the uninjured diaphyseal bone has relevance when normalising the strength of fracture repair in a limb when comparing it to the unfractured limb as frequently reported in animal studies of fracture repair.

In direct fracture healing bisphosphonate therapy resulted in impaired fracture healing as evident on plain radiographs based on the visibility of the fracture line. At six weeks post fracture the failure stress on application of a 4-point bend was decreased and histology revealed delayed bone healing compared to controls. Ibandronate treatment had an inhibitory effect on direct fracture healing in a rodent model.

In clinical practice, the treating surgeon may need to consider using non-rigid fixation methods in patients already on bisphosphonate therapy. When rigid fixation is essential patients on bisphosphonates will need to be monitored for features of delayed or non-union and the use of fracture healing adjuncts should be considered.

Thesis Declaration

The work in this thesis has been composed by myself and has not been submitted for any other degree or professional qualification. I have received assistance from individuals within our research group as indicated in the Acknowledgements.

Terence Savaridas

Presentations

Oral Presentations

Do Bisphosphonates Inhibit Direct Fracture Healing? **Savaridas T**, Wallace RJ, Gaston MS, Salter DM, Simpson AHRW. Winter Scottish Committee for Orthopaedics and Trauma (**SCOT**) Meeting, Crieff, Scotland, UK (Feb 2011). *Awarded 2nd Prize for Presentation.*

A Comparison of Fracture Healing with Rigid and Non-rigid Fixation in The Presence of Bisphosphonate Therapy. **Savaridas T**, Wallace RJ, Gaston MS, Salter DM, Simpson AHRW. International Society for Fracture Repair (**ISFR**), London, UK (Sept 2010).

Do Bisphosphonates Inhibit Fracture Healing with Plate Fixation? **Savaridas T**, Gaston MS, Wallace RJ, Salter DM, Simpson AHRW. British Orthopaedic Research Society (**BORS**), Cardiff, UK (Jul 2010).

Poster Presentations

The Effects of Bisphosphonate Therapy in Fracture Healing with Rigid Compression Plating. **Savaridas T**, Wallace RJ, Gaston MS, Salter DM, Simpson AHRW. International Society for Fracture Repair (**ISFR**), London, UK(Sept 2010).

Ibandronate Administered During Rat Tibial Fracture Repair Enhances the Bending Strength of Cortical Bone in the Uninjured Contra-lateral Tibia. **Savaridas T**, Wallace RJ, Dawson SP, Simpson AHRW. British Orthopaedic Research Society (**BORS**), Cardiff, UK (Jul 2010).

A Rodent Model of Internal Plate Fixation. **Savaridas T**, Muir AY, Gaston MS, Noble BS, Simpson AHRW. British Orthopaedic Research Society (**BORS**), Manchester, UK. (Jun 2008).

Contents

List of Figures

Fracture Healing

In the context of orthopaedic surgery a fracture is defined as a loss of continuity in bone. Fractures occur due to excessive force in traumatic injuries or following the application of a force consistent with normal activities on abnormal bone i.e. pathological fractures or as the result of repeated sub-yield forces in normal bone i.e. stress fractures.

The bone repair process during fracture healing is unique as it results in the restoration of the same tissue i.e. bone rather than a scar[1]. Fracture healing is a sequence of cellular events mediated by local factors that are influenced by the mechanical and physiological environment. It is an energy dependent process that involves a combination of bone resorption and deposition[1-3].

Fractures repair by two broad mechanisms. The mechanism of fracture repair that predominates is dependent on the stability and gap size at the fracture site[1].

Indirect Fracture Healing

The majority of fractures that are encountered in clinical practice are treated with non-rigid modes of fixation. With non-rigid fixation, indirect fracture healing occurs via bridging external callus with an intermediate phase of cartilage deposition. In this mode of fracture healing there may be an initial period of macromotion prior to a period of micromotion[4,5] between the fragments before solid union occurs.

Ham and Harris[6] in their textbook description of the histological appearance of indirect fracture healing based on rabbit studies of healing rib fractures elucidated the five stages of indirect fracture healing, namely;

1. Stage of haematoma

There is activation of non-specific wound healing pathways that accompany skeletal injuries. Haemorrhage from the bone ends lead to haematoma formation that is contained by the surrounding soft tissues. Degranulating platelets, macrophages and other inflammatory cells infiltrate the haematoma to[2];

i. prevent infection,

ii. secrete cytokines and growth factors,

iii. advance clotting into a fibrinous thrombus.

The rim of bone immediately adjacent to the fracture site is deprived of blood supply and becomes ischaemic. Non-viable necrotic cells and other debris are cleared by inflammatory cells[2].

2. Stage of cellular proliferation

Cytokines and growth factors recruit additional inflammatory cells in a positive feedback loop and also the migration of multipotent mesenchymal stem cells that are responsible for bone formation and repair[3]. Mesenchymal cells proliferate adjacent to the fracture site. A collar of active tissue, that predominantly consist of chondrocytes and fibroblast, is formed that surrounds each bone end and grows toward the other. Discrete cartilaginous regions grow and merge to produce a fibrocartilaginous, semi-solid, splint (soft callus) that provides early mechanical support to the fracture and will later serve as a template for bony hard callus formation[7]. It had traditionally been thought that osteoclasts were the key cell type for soft callus replacement and hard callus remodelling. Currently, it is suggested that soft

callus replacement is coordinated by multiple inflammatory cell types as part of a non-specific catabolic process and is less dependent on osteoclasts than the subsequent stage of bony hard callus remodelling[2]. This is supported by the observation that in osteopetrotic mutant strains of rats with deficient osteoclasts activity[8] and mice with decreased osteoclast number[9], there was no delay in the onset of hard callus formation and radiological union but a greater callus volume at 6 weeks post fracture. There was only a persistence of unmineralised cartilage in mice with near depletion or absence of osteoclasts throughout the duration of fracture healing[9]. This suggests that osteoclastic function is required but may not be the major factor for the process of soft callus remodelling. Alternatively a group of proteins known as matrix metalloproteinases (MMPs) that are secreted by a number of cell types including bone, cartilage and vascular endothelial cells are believed to be critical in soft callus remodelling. A decrease in MMPs has been shown to impede soft callus removal leading to delayed fracture union[10,11]. Colnot et al[11] demonstrated persistence of unmineralised cartilage in closed stabilised (external circular frame[12]) and non-stabilised[13] fractures of the tibia in MMP-9 deficient mice up to 21 days post fracture whereas mineralised hard callus was established by day 14 post injury in wild-type mice controls. Subsequently, in a similar study Behonick et al[10] observed impaired soft callus remodelling in MMP-13 deficient mice. MMPs also play a role in driving angiogenesis as observed in studies of solid tumour proliferation[14]. Angiogenesis is critical for the progression of fracture healing.

3. Stage of callus

This stage is characterised by high levels of osteoblast activity. Angiogenesis delivers osteoblasts along the semi-solid soft callus splint, initially at areas of stability along the periphery, and enables the removal of fibrocartilage and deposition of mineralised bone matrix[2]. The bone morphogenetic proteins (BMPs) stimulate the differentiation of osteoblast from osteoprogenitor cells[15]. Osteoblasts lay down new immature woven bone which forms the hard callus that is visible on plain radiographs. This bridge of callus imparts greater stability to the fracture. Of note, the osteoblasts secrete cytokines such as, Macrophage-Colony Stimulating Factor (M-CSF)[16] and Receptor Activator of NFκB Ligand (RANKL)[17], that are essential for the recruitment and function of osteoclasts that are present in increasingly greater numbers during the latter stages of indirect fracture healing[18].

4. Stage of Consolidation

The primary callus is transformed over time as a result of the orderly process of woven bone resorption by osteoclast followed by the formation of lamellar bone by osteoblast.

Bisphosphonates function primarily via osteoclast inhibition. Therefore, observations on the effects of bisphosphonate therapy during indirect fracture repair, provides information on relative osteoclastic activity within the stages of indirect fracture repair. In one study where bisphosphonate was only administered for two weeks pre-fracture[19] and in another where a single dose of bisphosphonate only was administered at one week post fracture[20] in a rat

diaphyseal fracture model, stress at failure and radiological union was not impaired at 6 weeks compared to controls. However, in experimental groups where regular treatment was continued for a period in excess of 4 weeks, which corresponds to the commencement of hard callus remodelling[20], the composition of woven to lamellar bone at the callus was greater at 4 months[19] and up to 6 months[20] compared to controls and rats that only received bisphosphonate treatment up to one week post fracture. The inhibitory action of bisphosphonate on osteoclast activity when administered during the period of hard callus remodelling in the rat led to a delay in the remodelling of woven bone to lamellar bone. This suggests that a high level of osteoclastic activity is necessary for the remodelling of woven bone to lamellar bone.

5. Stage of remodelling

   The bone is gradually strengthened along the lines of stress. The surplus collar of woven bone is gradually resorbed. Osteoclastic resorption creates erosive pits on the bone surface. New bone is then laid down in these pits by osteoblasts[2]. Bisphosphonate treatment has been shown to decrease the quantity of erosive pits[21].

Direct Fracture Healing

Direct healing occurs when the fractured ends of cortical bone are, rigidly held and closely approximated with a degree of compression[22-26]. The term 'direct' is used to denote the absence of an intermediate phase of connective tissue bridging the fracture site[1,3]. Direct healing can be considered to be an extension of the physiological repair and turnover of bone that is constantly occurring, whereby micro-cracks are located and removed by osteoclasts. New bone is then laid down by the ensuing osteoblasts following in the wake of the osteoclasts[22].

Direct healing was first noticed following the internal fixation of fractures. The earliest reported use of metalwork for internal fixation of fractures was by Carl Hansmann in 1885. Sir William Arbuthnot Lane used the term, "*as per primam intentionem*" to describe the radiographic appearance of absent callus in internally fixed fractures. Robert Danis in 1949 noted the importance of compression and stability at the fracture site to obtain direct healing, which he termed, "*soudere autogène*". These principles profoundly influenced the AO (Arbeitsgemeinschaft für Osteosynthesefragen) Foundation that has since been responsible for the burgeoning use of internal fixation to treat fractures with the goal of achieving early functional recovery[27].

The histological hallmark of direct healing is the osteonal remodelling unit tunneling across a fracture site at points of cortical contact in the presence of absolute stability[23-25,28,29]. This structure is known as a 'cutting-cone'. The head of the 'cutting-cone' primarily contains osteoclasts that resorb the dense cortical bone ahead as it travels toward and eventually crosses the fracture site. As the leading

osteoclasts migrate forward it leaves a trail that is immediately filled by new vessel ingrowth and osteoblasts that synthesise lamellar matrix on the pre-existing cortical walls[3] (Figure 1).

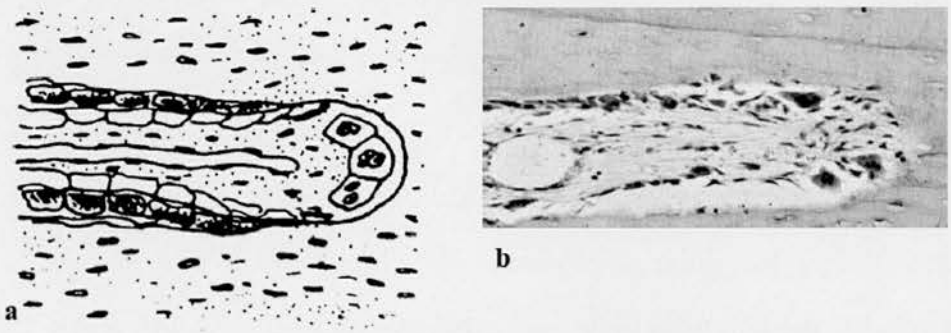

Figure 1: 'Cutting-cone'. (a) Schematic diagram shows cutting cone advancing from left to right led by multinucleated osteoclast which resorb bone followed by a central vessel and surface osteoblast synthesising lamellar bone. (b) Photomicrograph of cutting cone passing through rabbit cortical bone. ***From Shapiro F, European Cells and Materials 2008; 15: 53-76.***

The existence of the 'cutting-cone' is dependent on the fracture stability and ablation of the fracture gap achieved with close approximation of the fracture fragments. Of crucial importance to the healing process is an adequate blood supply to the fracture site.

Direct healing may also occur in the presence of stability and a minimal fracture gap. In this so called 'gap-healing' primary bone formation occurs, bridging the fracture gap, without an intermediate stage of connective tissue or fibrocartilage formation[1,23]. This newly formed bone does not initially correspond to the structure of the cortex. New bone is laid down by marrow derived vessels and mesenchymal cells parallel to the fracture line. Remodelling then occurs by osteonal 'cutting cones'

in the longitudinal weight bearing axis through the fragment ends across the newly formed bone within the gap[24-26,30].

The absence of woven bone formation and the immediate deposition of lamellar bone has been reported to occur in rigidly stabilised fractures in dogs[24,25]. Following rigid compression plating of transverse osteotomies in the dog radius Schenk and Willenegger[24] observed primary bone healing with 'cutting-cones' led by osteoclasts traversing cortical bone adjacent to the plate and gap healing on the far cortex where there was a fracture gap of 0.1mm. Olerud and Danckwardt-Lilliestrom[25] noted similar findings following rigid compression plating of dog radii and in the less vascularised dog tibia using the technique described by Schenk and Willenegger[24]. Perren[26] observed the same in rigidly plated sheep fractures with a fracture gap of less than 0.1mm. Direct fracture healing has also been observed in the rabbit[23,29].

Apart from the gap size the importance of stability has been stressed by several authors [23-25,28,29]. The need for stability is best described by the 'Strain' Theory[26]. This states that, "a tissue cannot be produced under strain conditions which exceed the elongation at rupture of the given tissue elements such as a cell". In the absence of an intermediate cartilage phase the tissues that bridge the fracture fragments are composed of bone that is relatively stiff. Therefore, minimal elongation of this small gap is likely to lead to rupture of the endosteal woven bone bridging the fracture. The tolerance to movement is least in small gaps as minimal motion causes a proportionally greater degree of strain of the tissues filling the gap.

Compression of the fracture fragments certainly contributes to the stability of fracture fixation as it helps to eliminate inter-fragmentary strain. Perren et al have

demonstrated that very small amounts of inter-fragmentary strain lead to bridging external callus formation. Inter-fragmentary strain values of up to 2% enabled direct fracture healing with no bridging external callus to occur in lamellar bone[22]. In routine clinical practice, when rigid modes of fracture fixation are used, it is unlikely that perfect anatomical reduction and abolition of the fracture gap is often achieved. However, it is likely that the fracture fragments are approximated with a degree of compression and the inter-fragmentary strain values within the existent gap is less than 2% therefore allowing fracture healing to proceed with no external callus.

With direct healing techniques, patient functional recovery is accelerated as load bearing though the injured bone can occur almost immediately following surgery. However, immediate mobilisation following fracture reduction is not confined to direct healing techniques and is also seen with non-rigid modes of fracture stabilisation such as intramedullary nailing of long bone fractures. In these instances, load is transmitted through the implant, therefore protecting the fracture reduction until bone healing is complete.

Anatomical reduction of articular fractures is enabled with open reduction and internal fixation hence avoiding abnormal areas of point contact at articular cartilage, which may prevent premature joint degeneration[31]. For these reasons, due to the enhanced functional recovery, and the predicted long term benefits of achieving anatomical reduction particularly at the joint surface, operative fracture fixation has become more common.

Summary of Fracture Healing

There are considerable differences in the processes involved between the two bone healing mechanisms. Osteoclasts are essential for the bone healing process, and their activity is known to increase at the fracture repair site. With indirect fracture healing via callus formation, osteoclastic activity peaks several weeks after the fracture[18,32], not during the early phase of fracture repair. In direct fracture repair, osteoclasts are of pivotal importance for the progression of 'cutting-cones' and therefore, are critical to initiate the process of direct fracture healing, Agents which impair osteoclast function, such as bisphosphonates may adversely affect the process of direct fracture healing.

Bisphosphonates

Structure & Function of Bisphosphonates

Bisphosphonate therapy primarily targets osteoclast function. Therefore, prior to describing the structure and function of bisphosphonates, a brief description is provided of osteoclasts formation, activation and mechanism of action. Osteoclasts are frequently a multinucleated cell, but may occasionally be mononucleated. Osteoclasts are derived from the haematopoietic cell line. They originate from the macrophage/monocyte lineage. Osteoclasts are formed from fusion of several precursor cells from the colony-forming unit (CFU) which can give rise to both granulocytes and macrophages. Multiple colony-stimulating factors (CSF) synergistically promote osteoclast formation however, the presence of M-CSF is essential. In mutations that lead to the absence of M-CSF production, osteopetrosis results, characterised by a paucity of osteoclast that is reversible by the administration of M-CSF[33]. The first visible step of bone remodelling is the focal attraction of osteoclast to the quiescent bone. Hormonal mediation, bone damage and cytokine release have been implicated in the stimulation of osteoclast activity[34]. The precise mechanisms by which osteoclast recruitment and activation occur are not fully understood.

The osteoclast is a highly energy dependent cell. It contains large numbers of mitochondria and lysosomes. Osteoclasts mediated bone resorption occurs following attachment of osteoclast to endosteal and periosteal surfaces creating a sealed off environment. At sites of osteoclast attachment to the bone surface a ruffled border is created by infolding of the osteoclast cell membrane. Within this sealed off area lysosomal enzymes are secreted and a local acidic environment is created by

operation of an ATP-driven proton pump. In this manner bone resorption occurs and an erosion pit is created. With ongoing resorption the osteoclast effectively tunnel their way in to mineralised bone. It is estimated that osteoclast may cut a depth of 20-25μm/day in mineralised bone[34,35]. The lifespan of osteoclast is between 4-12 days.

Bisphosphonates are synthetic analogues of pyrophosphate, an endogenous regulator of bone mineralisation. Bisphosphonates are comprised of two phosphonate (P) groups linked by phosphoether bonds to a central carbon (C) atom. This P-C-P structure is resistant to hydrolysis under acidic conditions and has a high affinity to divalent metal ions, namely Ca^{2+}, Mg^{2+}, and Fe^{2+} that are abundant in bone[36]. This enables targeting of bisphosphonate to bone mineral. There is an acidic environment at sites of osteoclasts mediated bone resorption[37] and bisphosphonates accumulate at these sites as bisphosphonates have a reduced ability to chelate divalent ions at low pH. The affinity of bisphosphonates to regions of low pH that correspond with sites of osteoclast activity facilitates bisphosphonate inhibition of osteoclasts mediated bone resorption. Bisphosphonates have been shown to be present in bone within 2 hours of administration[38]. In rat cortical bone, it accelerates osteoclast apoptosis and this is evident as a decrease in osteoclast number within 24 hours of drug administration[39].

Bisphosphonates may be divided into two distinct classes based on the predominant mechanism by which osteoclast mediated bone resorption is inhibited. The non-nitrogen containing bisphosphonates such as clodronate and etidronate are metabolised into non-hydrolysable analogues of adenosine triphosphate (ATP) that accumulate within osteoclasts leading to osteoclasts apoptosis. The newer more potent nitrogen-containing bisphosphonates such as ibandronate, risedronate,

zolendronate and alendronate are not metabolised. They inhibit key enzymes within the intracellular mevalonate pathway[40]. The mevalonate pathway is responsible for the generation of sterols and isoprenoid lipids. These cholesterols and lipids are important in osteoclast cell signalling. The isoprenoid lipids, in particular farnesyl pyrophosphate and geranyl-geranyl pyrophosphate, are essential for the prenylation and activation of small guanine transpherases (GTPases) such as Ras, Rho, Rac and Cdc42[40]. A decrease of these agents impair[36];

1. the formation of osteoclasts from osteoclast precursors
2. the recruitment and activation of osteoclasts
3. regulation of the osteoclast internal milieu.

This results in diminished osteoclast activity and may lead to osteoclast death by apoptosis[36,39]. Currently, the main target protein of nitrogen containing bisphosphonates is thought to be farnesyl diphosphate synthase (FDPS), a key regulatory enzyme in the synthesis of isoprenoid lipids[40]. In vitro studies using the J774 macrophage, which is frequently used as an osteoclast surrogate, have shown that nitrogen containing bisphosphonates inhibit protein prenylation within these cells and cause cell apoptosis[41,42]. However, addition of the isoprenoid lipids, farnesyl pyrophosphate and geranyl-geranyl pyrophosphate suppressed the bisphosphonate induced apoptosis in the J774 macrophage[42].

Statins act on the intracellular mevalonate pathway via inhibition of the enzyme HMG-CoA reductase. Laboratory studies suggest that statins enhance bone formation. A meta-analysis of randomised clinical trials that involved data analysed from more than 3000 patient did not however, demonstrated this class of drug to be as efficacious as bisphosphonates for the reduction of fracture risk[43]. This is likely

due to the lower affinity of statins to bone in comparison to bisphosphonates and therefore the effects of statins are less specific to bone.

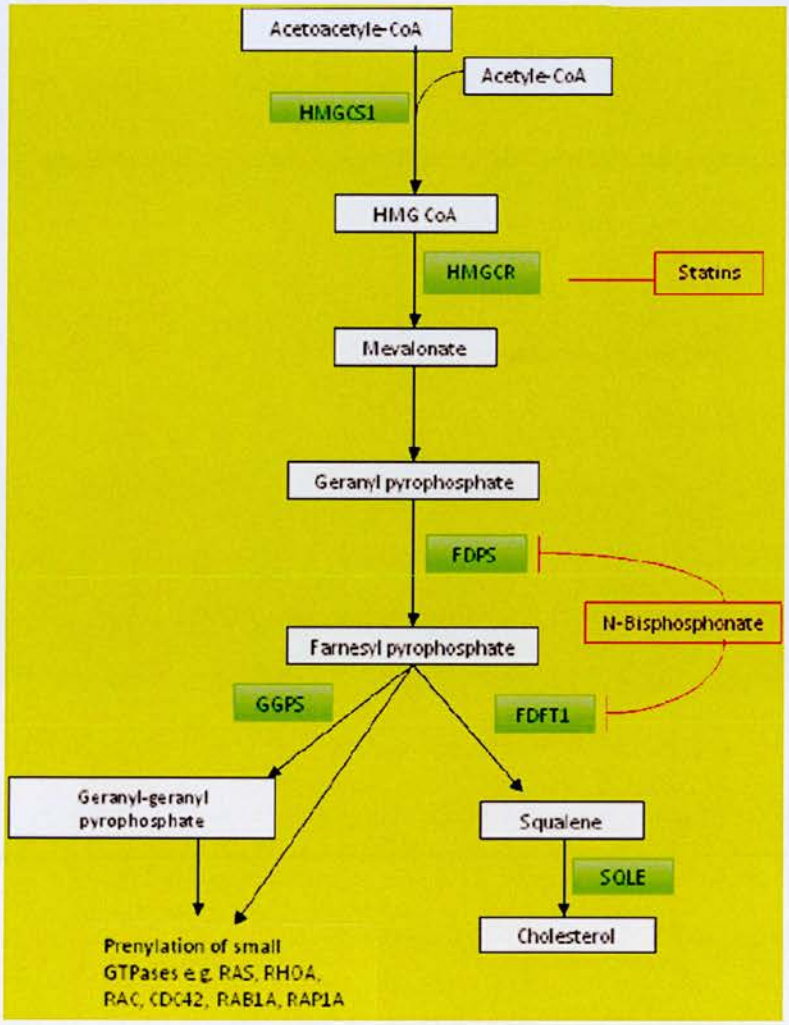

Chart 1: The intracellular mevalonate pathway. HMGS1, HMG Co-A synthase; HMGCR, HMG Co-A reductase, FDPS, farnesyl diphosphate synthase; FDFT1, squalene synthase; GGPS, geranyl-geranyl pyrophosphate synthase; SQLE, squalene epoxydase. (Adapted from Gong et al. Pharmacogenetics and Genomics 2011; 21: 50-53)

Nitrogen containing bisphosphonates are not metabolised and the proportion that is not adhered to bone surface is excreted unchanged through the kidneys. Oral

administration is recommended when fasting as food reduces the bioavailability of oral nitrogen-containing bisphosphonates[40]. The pharmacokinetics of bisphosphonates in humans is not fully understood. Bisphosphonate elimination is difficult to estimate as a proportion of bisphosphonate that adheres to the skeletal surface may be incorporated during new bone formation. A proportion of bisphosphonate re-enters the circulation following its physicochemical release from bone surface and following release during bone resorption. Therefore, the excretion of bisphosphonate is related to renal function and the rate of bone remodelling and turnover that in turn are affected by bisphosphonate activity. A prospective human study assessed renal excretion of bisphosphonate in eleven women with established post-menopausal osteoporosis for 18 months following intravenous administration of 30 mg alendronate given over four days. 50% of this was excreted in the urine within the first five days and the rate of excretion decreased thereafter. At six months 67% had been excreted and in the subsequent year only a further 3% was excreted. Therefore at 18 months, 30% of the administered dose was likely to still remain within the skeleton[44]. This skeletal retention may contribute to the prolonged duration of bisphosphonate effect.

Bisphosphonate effects within bone are not merely confined to osteoclasts. During the process of bone remodelling osteoclast activity is coupled to that of the osteoblast. This allows for tight regulation of bone deposition and resorption. Addition of osteoblast-like cells to osteoclast resorption pits in vitro are known to enhance bone resorption. In vitro studies following pre-treatment of these osteoblast-like cells with both nitrogen and non-nitrogen containing bisphosphonates before addition to osteoclastic pits lead to impaired bone resorption[21]. It is suggested that

bisphosphonates stimulate the release of a substance from osteoblasts that in turn inhibits osteoclasts mediated bone resorption[45]. Bisphosphonates have been shown to enhance bone marrow stromal cell proliferation and differentiation in to osteoblast in vitro[46], however it remains unclear whether bisphosphonates have a direct in vivo effect on proliferation of osteoblasts that results in enhanced bone formation[47].

Bisphosphonates in Clinical Practice

Bisphosphonates are an approved class of drug for the prevention of fragility fractures[48,49]. Clinical evidence on the efficacy of bisphosphonates in fracture prevention has been derived mainly from studies that demonstrate reduction in loss of postmenopausal bone mineral density (BMD) and decreased fracture risk, particularly in the vertebral column and femoral neck[50]. BMD measurements are a predictor of fracture risk. A meta-analysis of 12 randomised, placebo-controlled studies of antiresorptive drugs in postmenopausal women found that agents which produce a larger increase in BMD have greater anti-fracture efficacy[51]. Low BMD measurements are used to recommend antiresorptive therapies according to current national guidelines[48,49].

Prospective studies have shown that bisphosphonates prevent the loss of BMD[52-54] and recent randomised, double blind placebo controlled studies even suggests an actual increase in BMD[55,56] with corresponding decreased incidence of fragility fractures[52-54,57] in postmenopausal women. This evidence has led to the introduction of guidelines that recommend bisphosphonate therapy in patients with low BMD and following a single fragility fracture[48,49]. Subsequently, there has been an explosion in bisphosphonate uptake.

Currently, the United States Food and Drug Administration (FDA) have approved four bisphosphonates, namely ibandronate, alendronate, risedronate, and zolendranate for the treatment of postmenopausal osteoporosis. In placebo controlled randomised studies ibandronate has demonstrated promising efficacy in reducing the decrease in BMD and decreasing fragility fractures[54,57]. These results suggest that ibandronate, when administered in a once monthly oral regime, may be more

effective than other bisphosphonates as demonstrated by gains in lumbar spine and hip BMD[50]. Furthermore, ibandronate has been shown to prevent fragility fractures when administered orally using an intermittent dosing regimen[54]. Bisphosphonates are associated with significant upper gastrointestinal symptoms and this may reduce compliance. The convenience of an intermittent oral dosing regimen in addition to its reported efficacy suggest that ibandronate may be a preferred bisphosphonate for fracture prevention, hence its use in this study.

The Effects of Bisphosphonates on Fracture Healing

Animal Studies

The effects of bisphosphonates on indirect fracture repair via callus formation has been extensively studied in laboratory animals. Animal studies on rats[19,20,32,58-67], sheep[68] and dogs[69,70] have revealed no adverse effects of bisphosphonates, at doses used to prevent post ovariectomy associated loss in bone mineral density (BMD), on the restoration of mechanical integrity of healing fractures. The physical properties of the healing fractures following bending, tensile or torsional stress are either enhanced[19,32,58,59,61,62,68,69] or remain unchanged[20,64,66,67] in comparison to controls. Generally, an increase in physical strength at the fracture site in bisphosphonate treated animals was noted in conjunction with the observation of greater callus volume on radiological assessment[19,32,58,59,61-63,65,67,68,70]. However bisphosphonate therapy in beagle dogs[70] and rats[20,67] respectively had no effect on bending strength of mid-shaft diaphyseal fractures despite the larger callus width noted on plain radiographs. This suggests that the callus formed following bisphosphonate therapy may have impaired physical properties but strength at the fracture site is compensated for by the structural properties that are provided by a bulkier callus volume.

The callus composition in bisphosphonate treated animals appears to have a lower mineral content[65] and a greater proportion of woven to lamellar bone[19,20,32,59], suggesting a delay to the process of callus remodelling[19,20,67,68,71] in indirect fracture healing. There appears to be a dose dependent effect on callus remodelling with

higher doses of bisphosphonates having a greater effect on decreasing callus mineralisation[69].

The timing of bisphosphonate therapy relative to the fracture process affects bone repair. In a rat femoral fracture model, bisphosphonate administration up to one week post fracture did not affect radiological union or failure stress at six weeks[19,20]. However, in groups where regular bisphosphonate treatment was continued for longer periods post-fracture, i.e during the commencement of hard callus remodelling[1,20], there was a greater proportion of woven to lamellar bone within the callus at four months[19] and up to six months[20] compared to healthy controls and rats that only received bisphosphonates up to the first week of fracture healing.

The callus characteristics and rate of remodelling are related to the bisphosphonate concentration and the bisphosphonate inhibitory effect on osteoclasts within the healing bone. High doses of bisphosphonate have been shown to adversely affect the mechanical strength of healing fractures in dogs[69].

It is known that there is heightened osteoclast activity at sites of bone repair. A recent study using a sheep tibial osteotomy stabilised with an external fixator showed that the osteoclast numbers at the fracture site gradually increased during the duration of indirect fracture healing with a sharp rise after three weeks[18], that may indicate osteoclasts importance in the callus remodelling phase that begins between the third and fourth week post fracture[1,20].

Following administration of a single dose of zolendronic acid to healing rat femoral fractures, Amanat et al[32] found larger callus volumes, and increased mechanical strength in torsion at the fracture site with evidence of delayed remodelling when the single dose was delivered at one and two weeks post fracture compared to at the time

of fracture. A greater effect was noted in the two weeks post fracture group. Furthermore, the concentration of zolendronic acid was greatest within the callus of the delayed treatment group due to the high affinity of bisphosphonates to areas of osteoclast activity which would have been greater at this time point.

As mechanical integrity is critical to functional recovery and rehabilitation post fracture, delaying the onset of bisphosphonate therapy following fragility fractures may be clinically beneficial. The longer term effects of this delayed callus remodelling remains uncertain but studies of healing fractures in sheep up to 3 months[68], dogs to 5 months[69] and rats up to 12 months[62] show no adverse effect on mechanical strength.

A recent study by Bauss et al[72]assessed the healing of drill holes in beagle dog tibiae following administration of systemic ibandronate therapy. Ibandronate administration did not adversely affect the amount of newly formed bone within the defects. It was however, assessed in the presence of ipsilateral femoral marrow ablation. Bone marrow ablation has been shown to enhance osteogenesis at distant sites and this may have had a confounding effect on the results. In a study using aged rats there was a significantly greater thickness in the zone of provisional calcification, the site at which osteoblastic bone formation occurs, of the mandibular condyles within 6 days following tibial marrow ablation through a drill hole in comparison to controls where a tibial drill hole only was made without marrow ablation[73]. Furthermore, drill hole defects do not replicate the clinical scenario of primary fracture repair.

Contrastingly, in a rabbit calvarial defect model pamidronate therapy was observed to impair angiogenesis and resulted in a greater proportion of fibrous tissue to bone

formation within the defect at 8 weeks[74]. This suggests that via an inhibitory action on angiogenesis bisphosphonates may impair primary bone formation.

Human Trials

There have been two prospective randomised double-blinded, placebo controlled clinical studies that assessed the bone mineral density (BMD) in the region of healing distal radius fractures treated non-operatively[75,76]. Both studies investigated post-menopausal women that were commenced on alendronate[76] and clodronate[75] respectively following fracture and followed up to 12 months. The clinical and radiographic assessment of fracture union was not affected in both studies. The authors concluded that the bone mineral density was greater in the bisphosphonate treated groups at the fracture site, thereby suggesting that bisphosphonate therapy prevents the loss in bone mineral density associated with fractures. However, impaction of the fragments, as frequently occurs in wrist fractures may have led to increased BMD measurements locally in the region of the healing wrist fractures and therefore confounded their findings. Furthermore, as no measurements were made of the callus size the rise in BMD could be related to a larger callus bulk as previously demonstrated in animal models of indirect fracture healing with bisphosphonate treatment.

The longer term effects of bisphosphonate therapy especially on cortical bone, requires further study. This is especially relevant in light of emerging clinical reports of low energy diaphyseal fractures[77-79] and subsequent delayed healing[78] as observed on radiographs in patients on long term continuous alendronate therapy of between three to eight years.

Summary of Bisphosphonate Effects on Fracture Healing

A number of studies have reported that during indirect fracture healing, bisphosphonate therapy delays callus remodelling and prevents fracture associated decrease in bone mineral density. The delay in callus remodelling results in a callus of poorer mechanical property but this is associated with a larger callus volume that compensates for the strength at the fracture site.

As direct fracture healing proceeds through different biological processes it is not possible to extrapolate from previous research, that either used non-rigid stabilisation or bone defect models, the effect of bisphosphonate therapy on direct fracture healing. As osteoclasts are of pivotal importance for the initiation of the progression of osteonal remodelling units that are essential at the onset of direct fracture healing, bisphosphonates may have a detrimental effect on direct fracture repair.

Bisphosphonate Effects on Bone Remodelling

The promising effectiveness of bisphosphonates in fragility fracture prevention occurs at the expense of decreased bone remodelling[71,80-82]. In a one year placebo-controlled study using adult beagle dogs, comparing two nitrogen-containing bisphosphonates at six times the recommended therapeutic dose, Li et al.[71] reported more 'microcracks' and a reduced association between 'microcracks' and osteoclasts resorption sites in bisphosphonate treated dogs. The impaired bone remodelling, resulted in microdamage accumulation. One year of alendronate therapy, at the treatment dose shown to reduce the incidence of fragility fractures, in a placebo controlled human study revealed decreased plasma biochemical markers of bone turnover[80], which may be a reflection of reduced bone remodelling. In dogs microdamage accumulation at 3 years following alendronate therapy was not significantly different to that observed following one year of similar therapy, however the bone strength following adjustment for BMD was reduced in the alendronate treatment group compared to controls[82]. Recent clinical evidence has emerged that suggests an association between low energy diaphyseal fractures and long term nitrogen-containing bisphosphonate therapy[77-79]. Bone biopsies revealed severely reduced surface osteoblast and low surface osteoclast numbers with suppressed new bone formation[78]. This suggested that long term bisphosphonate therapy impaired the recruitment of both osteoblast and osteoclast to the site of bone damage. This may lead to accumulation of microdamage and subsequent crack propagation leading to fracture.

Direct fracture healing that predominates in plate fixation can be considered an extension of the normal physiological processes involved in bone turnover and

remodelling, where bone microdamage is identified and repaired. The growing evidence that bisphosphonates inhibit bone remodelling support the hypothesis that bisphosphonates may have a detrimental effect on the process of direct fracture healing.

Bisphosphonate Effects on Cortical Bone

Animal trials in rodents, canines and primates have consistently shown that bisphosphonate increases the compressive load at failure of cancellous bone within the vertebra[83-88] and femoral neck[83,84]. Prospective human studies[50,52-54] show that bisphosphonates prevent loss of BMD and decrease fracture risk particularly in the vertebral column and femoral neck with recent randomised, double blind placebo controlled clinical studies[55,56] even suggesting an actual increase in BMD with once monthly oral bisphosphonate.

However, studies that demonstrate an increase in cancellous bone compressive strength and preservation of BMD with bisphosphonate therapy have not shown consistent effects on diaphyseal bending strength[83,89]. The effect of bisphosphonates on cortical bone mechanical properties, particularly of the uninjured contra-lateral cortical bone remains poorly reported.

This is of particular importance as cortical bone remodels less quickly than cancellous bone and bisphosphonate inhibition of remodelling may lead to accumulation of 'microdamage' [71] that may manifest clinically as cortical insufficiency fractures[77-79].

Following a fracture a decrease in bone mineral density occurs both within the injured limb[76] and in the contra-lateral uninjured limb[90]. The effect of bisphosphonate administration during the fracture healing process on the radiological density and mechanical properties of the uninjured diaphyseal bone in the contra-lateral limb has not been studied to date.

Animal Models of Fracture Healing

Animal fracture models have been extensively used in pre-clinical studies of fracture healing. The choice of animal used is mainly influenced by the following:

1. Intervention to fracture repair being assessed e.g.
    a) method of fracture stabilisation
    b) systemic or local pharmacological agents (e.g. bisphosphonates, bone morphogenetic proteins, synthetic bone graft)
    c) systemic or local disorders that may influence bone repair (e.g. osteoporosis, diabetes mellitus, immunodeficiency, limb paresis)
    d) exogenous agents (e.g. ultrasound therapy, electrical stimulation)
2. Method of analysis to determine progression of fracture repair e.g.
    a) biomechanical testing
    b) histological analysis
    c) immunohistochemistry
3. Similarity of animal model to clinical environment
4. Animal handling cost
5. Availability of genetically modified models, e.g. knockout mice
6. Societal acceptance of a particular animal species being used for research

Animal models to study fracture repair have been described in; small animals such as mice[12,13,91-95], rats[96-103] and rabbits[6,23,29,30,104]; domestic animals such as cats[105] and dogs[25,106]; larger animals such as sheep[28,107] and horse[108]; and in non-human primates[109,110].

In general, small animal models, especially in the mice, have been used to study the molecular aspects of fracture repair. Understanding of the mouse genome has

enabled fracture studies to be performed on genetically modified strains that display phenotypic traits of a particular disorder. The low cost of purchase and upkeep for mice in addition to the substantial understanding of the mouse genome make it an increasingly common choice for fracture healing studies[111,112]. Surgical stabilisation of fractures in small animals is technically demanding and biomechanical testing of small bone specimens is difficult[113]. Experiments that investigate the mechanical properties of surgical stabilisation devices for fracture repair and that have a focus on assessing the biomechanical environment of fracture repair frequently use larger animal models. The classical descriptions of direct fracture repair were based on rigid plating of osteotomies in the dog[24,25] and sheep[28]. Direct fracture healing has also been observed following rigid plating of tibial osteotomies in the rabbit[23].

The properties of bone and its response to loading and fracture have differences between animal species. It is believed that the closer a species is on the phylogenetic scale the similarities would be greater[112]. Animal models are essential for the study of fracture healing. However, the observations made in one animal species may not be identical to that seen in another species or in human studies.

It is often stated that bone remodelling does not occur in the rat[111,112]. However, Bentolila et al[114] axially loaded the right ulna in sixteen adult rats, then ten days later loaded the contra-lateral ulna prior to immediate sacrifice. They observed that the right, earlier loaded, ulna diaphysis had 40% less 'microcracks' than the contra-lateral ulna diaphysis that was loaded immediately prior to sacrifice. On confocal microscopy of fuchsin stained bone sections there was cortical remodelling near'microcracks' and intracortical resorption associated with osteoclastic tunnelling. This suggests that the 'microcracks' are being repaired by a process of bone

remodelling. This observation led us to suspect that direct fracture healing may occur in the rat provided that there is anatomical fracture reduction and a biomechanical environment of absolute stability to permit progression of 'cutting cones' across the fracture site. A rodent model of direct fracture healing has not been previously described.

In the following section a summary of frequently used small animal models of fracture healing is presented.

Small Animal Fracture Models

Mouse Fracture Models

Its small size renders surgical procedures to be difficult. Closed tibial diaphyseal fracture models have been described using variations of a guillotine device[12,13,91]. Bourque et al[13] reported in a closed tibial fracture model with no immobilisation that fractures healed with endochondral ossification within 21 days. Hiltunen et al[91] inserted 0.2mm stainless steel rods into the tibial intramedullary canal bilaterally in 68 mice prior to creation of a closed fracture. Nine animals died during the perioperative period and one developed an infection. Malposition of the intramedullary rod was reported in only one of the remaining 116 fractures. Fractures healed by endochondral ossification with visible external callus on radiographs. Thompson et al[12] described a model of fracture healing via intramembranous ossification in the mouse tibia following external fixation of a closed tibial fracture with a circular frame. The frame consisted of two aluminium rings stabilized by threaded rods secured to the proximal and distal tibial metaphyses with smooth cross pins. This produced a more stable construct and prevented rotation of the fracture ends when compared to an intramedullary rod. A small amount of cartilage was detected on immunohistochemistry by detection of CoIIIa, a marker of chondrogenesis, at two weeks, but not at earlier time points at days 4 and 7, in four of ten animals. At three weeks there was woven bone bridging the fracture site with external callus on radiographs. The cartilage noted may be due to instability of the frame construct by three weeks either due to loosening at the interface between the smooth pin and metaphyseal bone or the aluminium ring. In the three models

described above, where closed fractures were created with a guillotine device, there was no mechanism to prevent an associated fibula fracture (1/3 of animals reported by Thompson et al[12]).

There are two described models of murine femoral osteotomies stabilized with uniaxial fixators whereby healing occurred by endochondral ossification[93,94]. In the model by Connolly et al[93] a drilling jig with a greater distance between the proximal and distal holes was used to permit compression of the fracture on external fixator bar application. In this study animals were individually housed in cages fitted with an infra-red beam motion detection system. They observed, animals that were more active had larger external callus.

Recently, Histing et al[92] described a mouse femoral osteotomy model stabilized with a locking plate whereby fracture healing progressed via intramembranous ossification. A transverse femoral osteotomy was made with a 0.22mm diameter Gigly saw. A 4-hole 1.5 mm thick titanium plate was used. In 4 (20%) of 20 animals there was intra-operative failure of plate fixation. At two weeks, eight animals were sacrificed. On trichrome staining they observed callus of woven bone with no cartilage. At five weeks there was radiological union and on histology there was woven bone bridging the fracture in all of the eight remaining animals. Cutting cones were not observed to traverse the osteotomy site in this model

A cortical drill hole model in the mouse tibia has been reported[95]. Within one week of a 0.5mm tibial drill hole woven bone was observed in the defect with some periosteal cartilage at the periphery of the defect. New woven bone filled the marrow cavity defect by four weeks post injury.

Rat Fracture Models

The closed rat femoral fracture model by a guillotine device following intramedullary retrograde reaming with a 20 gauge needle and femoral stabilisation with a 0.45 mm diameter Steinmann pin was originally described by Bonnarens and Einhorn[97] in 1984. It has been widely used for fracture healing studies in the rat femur and subsequently adapted for use in the tibia of rats[98] and mice[91]. Bonnarens and Einhorn[97] observed that in 38 of 40 animals there was a transverse fracture in the middle third of the femur diaphysis. In a further two the fracture in the femur diaphysis was of a transverse oblique pattern. Therefore the guillotine device was able to reproduce a standardised closed fracture. However this device when used in the tibia often created a concomitant fibula fracture but was able to reproduce a standardized rat tibial diaphyseal transverse fracture in 159 of 176 animals[98].

Bak et al[115] produced a closed tibial diaphyseal fracture following application of a 3-point bend with a specially designed forceps. A smooth intramedullary K-wire was then introduced across the fracture. The aim of this study was to assess the effect of the fracture level on the mechanical properties of the healing fracture. The failure load and stress decreased with more distal fractures. The authors concluded that this was likely related to less support provided by a correspondingly more distal fibula fracture that will not be embedded in muscle distally in the leg and also due to the shorter working length of the intramedullary K-wire across the fracture site in lower tibial fractures. This study emphasised the importance of fracture standardisation.

Rat femoral osteotomy models stabilized by an intramedullary pin[101] and with an external fixator[103] have also been described. Russell et al[96] described femoral plating with a 1mm thick stainless steel plate in the rat femur followed by osteotomy of a 5

mm segment of bone to create a critical size defect segmental non-union model with rigid fixation.

Rabbit Fracture Models

Rahn et al[23] reported direct fracture healing following rigid stainless steel dynamic compression (DC) plating of eight adult rabbit tibial osteotomies. The site of osteotomy in the tibial diaphysis was stripped of periosteum, for a length of greater than twice the diameter of bone at the osteotomy site, prior to sawing with a handsaw of 0.1mm thickness under constant cool saline irrigation. A 6-hole plate was used. In three of eight animals the screws holding the plate had loosened. The ensuing instability resulted in resorption of the fragment ends and development of interfragmentary cartilage with bridging callus. In five animals with rigid fixation, 'cutting-cones' were seen to traverse the osteotomy site on the surface beneath the plate with no evidence of interfragmentary resorption (i.e. contact healing). In the cortex opposite to the plate where a small gap occurred, new bone formed parallel to the osteotomy line with 'cutting-cones' crossing the gap perpendicular to the osteotomy site (gap healing). This histological appearance is similar to that reported in the dog[25,106,116] and sheep[28]. The observations of Rahn et al[23] were reproduced by Ashhurst et al[29] in 24 of 29 similarly DC-plated rabbit tibia. In four animals there were fractures around screw holes resulting in instability and one animal died under anaesthesia. However, when the fragments were approximated, within 0.5mm to 1.0mm, and stabilized with a less stiff plastic plate indirect fracture healing occurred with external callus.

Brighton et al[104] used a transverse midshaft fibula osteotomy to assess the effect of capacitively coupled electrical fields on fracture repair. No fixation or external immobilisation was used as the fibula is synostotic to the distal tibia. Fracture repair occurred with intermediate cartilage formation and bridging callus on histology.

Choice of Animal Fracture Model

Rigid plate fixation in the mice is difficult due to the small size of bone. A model of locking plate stabilisation in the mouse femur did not produce absolute stability to permit direct fracture healing[92]. Haversian remodelling is known to occur in the rat[114]. It was therefore reasoned that direct fracture healing was likely to be observed in the rat under suitable conditions. Based on this the rat was chosen as the animal model for this research. Furthermore, the animal cost for purchase and handling of rats is at least three times less than that for a larger animal such as the rabbit at the University of Edinburgh animal research facilities.

The tibia was preferred to the femur as surgical approach was more direct and positioning for serial x-rays to assess the progression of fracture healing would allow greater standardisation. As a surgical approach would be required for plate fixation an osteotomy model was used as this allowed for standardisation of the 'fracture' and avoided a concomitant fibula fracture which may impair the mechanical properties of healing non-rigidly stabilised tibial fractures in the rat[117,118].

The Assessment of Fracture Healing

Both functional and imaging techniques were used to assess fracture healing.

Mechanical Testing

Bending stress has been widely used in previous studies to assess the mechanical properties of healing fractures in rodents[19,59,62,64,119] and therefore the results gathered from this research would be comparable to evidence in the published literature. Bending causes tensile stresses on the convex surface and compressive stresses at the concave surface. 3-point bending tests have been used by several authors to assess the mechanical properties of healing fractures in the rat[67,99,120,121]. This is likely due to the ease of testing especially in small bone specimens.

A four-point bend is superior to a three-point bend as it produces pure bending between the two middle loading points and ensures that transverse shear forces, which are not measured, are eliminated[113,122]. This produces a more accurate measurement of the failure load and has previously been used to measure the failure load of healing mouse tibial fractures[91].

Alternatively, testing bone mechanical properties with pure tensile force can yield highly accurate measurements, but this method of testing requires relatively large specimens that are able to be shaped to create a design where the majority of strain will occur in the mid-portion of the specimen during the application of a uniaxial tensile force[113]. Hence, this method was not suitable for use in small rodent bones. Testing in pure compression is particularly useful for testing small specimens. It was less accurate due to end effects on the bone during testing that was most marked in smaller specimens[113].

Several authors have used testing in torsion[118,123] to report on mechanical properties of healing fractures in rodent bone. However, testing in torsion produces tensile stress in addition to shear stresses that were difficult to quantify accurately[124]. Pure shear test of bone requires bone of specific shape and size that would be difficult to obtain from rodent bone[113].

Four-point bending stress was used as it bears resemblance to the mechanics of tibial fractures seen in clinical practice and the material properties can be accurately measured by using the "Elastic Beam Bending Theory" as will be described later.

Specimens require adequate storage and preparation to enable accurate mechanical testing. Tissue autolysis of bone is known to begin early following specimen retrieval[125]. As this may have affected the mechanical properties of bone, it was vital that specimens were adequately stored to prevent this process. It has been shown that freezing specimens at -20˚C in isotonic saline solution for 3-4 weeks prior to bending test does not affect the strength of human cortical bone when compared to controls tested in similar conditions immediately following retrieval[126]. This method of storage by freezing in saline, prior to mechanical testing has been widely used in previous experiments to assess the effects of bisphosphonates on fracture healing in rodents[32,58,61,64,119] and was therefore used in this thesis.

The mechanical properties of bone are affected by temperature and moisture[113]. At temperatures below 27°C bone fails at a lower stress and at warmer temperatures there is a larger degree of plastic deformation prior to failure that results in an apparent greater stress at fracture[127]. Bone when dehydrated behaves in a more brittle manner[113]. Therefore mechanical testing of specimens were performed whilst the bone was still hydrated and warm. This was to maintain bone hydration and

temperature close to 37°C in an attempt to simulate bone properties in vivo and to standardize testing conditions for all specimens.

Radiography

Serial Radiographs

This is a simple method to monitor the progression of fracture healing. The process of direct fracture healing was first considered following observations of fracture repair without external callus on serial radiographs[27]. Clinicians routinely monitor fracture healing with serial radiographs. Fracture alignment, visibility, callus formation and fixation are qualitatively assessed.

Callus Index

Callus index in healing tibial diaphyseal fractures is defined as the ratio of the maximum callus diameter to bone diameter at the similar level as the callus[128] (Figure 21). The callus size increases until stability is achieved across the fracture site prior to commencement of callus remodelling[6].

The influence of callus size on fracture healing strength was noted by Lindsay and Howes[129] in a rat study of standardised fibula fractures without immobilisation. They noted that there was a peak in load at failure of healing fractures at day-21 that corresponded with the peak in callus size. After day-21 there was a period of decline in the failure load of healing fractures and also a decrease in callus size prior to a secondary rise in strength at the fracture between day-33 and day-45 as the callus size continued to decrease to its pre-fracture bone diameter. These radiological observations of callus size are in agreement with subsequent histological studies of healing rat fractures whereby the callus size is noted to decrease and remodel between the third to fourth week post fracture[20]. Within the clinical environment,

this similar observation has been noted in a prospective clinical study of seven patients with non-comminuted tibial fractures treated with uniaxial external fixators. Gardner et al[5] observed that the callus index increased in relation to an increase in stability at the fracture site.

Eastaugh-Waring et al[128] in a retrospective study of three groups of 15 patients each with tibial fractures that were treated with cast immobilisation, intramedullary nail fixation or external fixation observed a sharp rise in callus index in the early weeks post fracture, with a flattening of the curve prior to reaching a peak callus index and a subsequent decrease in all three groups. The peak in callus index occurred shortly after cast and external fixator removal suggesting that monitoring this radiographic measure may indicate progression of fracture stability and help advise patients on returning to function.

It has been suggested that serial callus index measurements in non-rigidly stabilised healing tibial fractures peak at a point that coincides with callus remodelling[128]. Therefore serial callus index measurements enabled assessment of the initiation of callus remodelling and progression to fracture consolidation.

Visibility of Fracture Line

This method has been used in the assessment of experimental fracture healing in the rat[61]. In a study to assess the dosing effects of a systemic agent on closed tibial fractures in 40 adult goats stabilised with external fixators, weekly standardised radiographs were obtained up to the point of animal sacrifice. Soft tissues were dissected prior to contact radiographs and mechanical testing. All radiographs were reported by two independent radiologists who were blinded to the treatment that the

animals received and the time point from fracture that radiographs were taken. The visibility of the fracture line was scored on a 3-point scale as either; absent, partially disappeared or visible. The findings were that this method of assessing fracture line visibility had good inter-rater agreement and good correlation with mechanical testing data[130].

Histology

This allows for assessment of the general morphology at the fracture site. In order to obtain sections of bone with optimum preservation of cellular architecture samples are fixed in formalin, decalcified and embedded in paraffin.

Formalin is routinely used for tissue fixation as it preserves tissue morphology with few artefacts, is cheap, easy to prepare and is used widely[131]. Formalin fixation involves the development of protein cross-linking and the formation of co-ordinate bonds for calcium. Forty-eight hours is accepted as sufficient for tissue fixation as the quantity of tissue fixation plateaus after this period[131,132]. Delayed commencement of fixation (>30min) results in increased proteolytic degradation and prolonged fixation (>48hrs) results in excessive protein cross-linking which alters the protein structure and may adversely affect the quality of specimen staining[131].

Bone requires decalcification prior to embedding in paraffin to permit sectioning. Removal of calcium and resulting dissolution of hydroxyapatite can be achieved by strong acids or chelating agents. Acids such as nitric, hydrochloric and formic acid achieve rapid decalcification at the expense of hydrolysis of nucleic acids and denaturing enzymes but may hinder subsequent assays and immunohistochemical techniques[133]. Therefore bone specimens are decalcified in a chelating agent, disodium ethylenediamine tetraacetic acid (EDTA). Decalcification of bone with EDTA as initially described by Nikiforuk[134] is still regarded as the most suitable technique for the preservation of tissue architecture[133].

To permit comparison it is important that the bone sections produced for analysis from each sample are standardised, reproducible and representative of the entire sample.

Hypothesis, Aims and Clinical Relevance

Hypothesis

1. A model of direct fracture repair can be developed in the rat.
2. Bisphosphonates inhibit the process of direct fracture healing (as this is 'led' by osteoclasts) but not that of indirect healing.

Research Question:

Does ibandronate (a nitrogen containing bisphosphonate) therapy inhibit direct fracture repair in the rat?

Specific Aims

To investigate the effect of a systemically administered bisphosphonate on the process of direct and indirect fracture healing in diaphyseal fractures stabilised rigidly using plate fixation or non-rigidly with an external fixator using clinically relevant fracture models.

Null Hypothesis: Ibandronate has no affect on fracture healing in-vivo

Clinical Relevance:

The results of this study will guide the orthopaedic surgeon in their choice of fracture fixation technique for the management of the growing number of osteoporotic fractures in patients already on bisphosphonate therapy. The findings will be of particular relevance, to advise whether orthopaedic surgeons should use rigid stabilisation methods in patients on bisphosphonates.

Development of Animal Models

All animal procedures adhered to the Animals (Scientific Procedures) Act 1986 and were approved by the appropriate local and national authorities. Animals were fed standard rat chow and provided with water ad libitum. Animals were housed in individual cages at constant temperature (21 ± 1°C) and humidity (45% - 55%) using a 12 hour light/dark cycle. Surgical procedures were only commenced after one week of housing to allow for acclimatisation to their new environment. Techniques and implants were initially trialled in rat cadavers prior to application in experimental animals.

Rat Model of Direct Fracture Healing

The model of tibial plating used in this study was developed with reference to a model of plating rat femoral shaft osteotomies[96]. This previously described technique was used to obtain rigid internal fixation at the fracture site, thus enabling healing without callus. However, it was designed as a model of femoral non-union with an osteotomy gap of 5mm in order to evaluate compounds that will enhance primary bone formation while eliminating the effects of callus formation. Therefore, adaptation was required to develop a model of direct fracture repair, similar to that seen in clinical practice when open reduction and internal fixation is achieved by using compression plate fixation.

The tibia was chosen as it had a suitable flat surface medially which enabled positioning of a plate on to bone. The use of two screw holes on either side of the fracture site was maintained, as this was the minimum number of fixation points required to obtain rigid stability in all planes.

Essential to this model of fixation was the development of the following materials:

- Hardware for internal fixation
- Jig for positioning of screw holes to ensure apposition at fracture site on plate application
- Cutting device for osteotomy

Based on repeated measurements of 22 extricated tibia from eleven adult male Sprague-Dawley cadavers with a mean (±SD) weight of 496 (±46.1)g, the average tibial dimensions were as follows:

Tibial length	Sagittal width at narrowest point distal to fibula insertion	Tibial midshaft coronal width
43.0(±1.2)mm	3.1(±0.2)mm	2.89(±0.12)mm

Table 1: Mean (±SD) tibial dimensions from cadaver rat tibia

These values correspond with adult rat tibial dimensions as previously observed[121,135].

1.6 mm diameter threaded screws were chosen as these were readily available in the 4mm length required. A screw of 1.6 mm diameter would still leave just under 50% of the sagittal bone width intact at the narrowest point should the plate be inserted distally on the tibia. A 4 mm length was required to ensure there was purchase on the lateral far cortex during screw insertion especially with the proximal screws, as the tibia is thicker in the coronal plane proximally. The plate thickness was chosen at 1mm as per described in the femoral plating model[96]. The initial plates were made to a length of 16 mm and width of 4 mm to accommodate four 1.6 mm screw holes. All metal-ware was stainless steel due to its favourable combination of mechanical properties, biocompatibility, corrosion resistance and cost effectiveness.[136] These properties allowed provision of adequate rigidity to achieve absolute stability at the fracture site and prevented adverse antigenic reactions.

A trimmed junior hacksaw blade with a width of 0.5 mm (RS Components, UK) was chosen to create the osteotomy. This was to reduce thermal necrosis of bone that may be produced by the use of high speed oscillating saws in the absence of irrigation[137]. A 1.25 mm drill bit powered by a hand held Dremel® Multitool was used to make 4 screw holes in the bone. A custom made 4-hole jig was used as a

guide to drill the bone. The spacing between the 2nd and 3rd hole on the jig was 0.5 mm greater than the space between the corresponding holes on the plate. This was to ensure apposition at the osteotomy site during plate fixation. The jig had a roughened inferior surface to prevent sliding on the bone surface and holes on the lateral surface to thread a fine wire to secure the jig to bone during drilling. The jig height was 4mm and the four-holes were of 1.25mm diameter to ensure a tight fit with the drill bit to obtain accurate positioning and alignment of the drill holes. Once 4-holes were drilled in bone and tapped with a M1.6 fluted tap, the osteotomy was created with the previously mentioned saw blade. The plate was then applied and secured with 4 fully threaded 1.6mm screws. Tightening of the screws caused apposition at the fracture site (Figure 2).

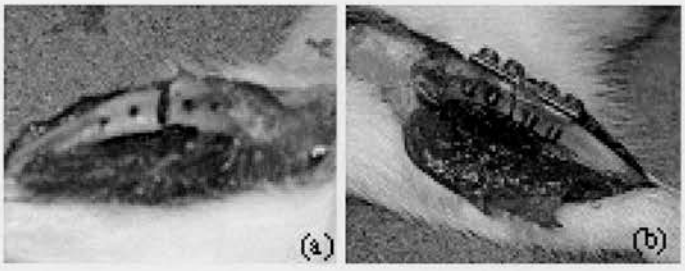

Figure 2: (a) Transverse osteotomy in pre-drilled bone and (b) apposition at osteotomy site

Following successful application on ten rat cadaver tibiae, this plate was used to fix tibial osteotomies, initially in two adult Sprague-Dawley rats. The osteotomies were created at the proximal diaphysis of the tibia to allow the placement of 4 screws in areas where the tibia remains wide. Unfortunately, as the proximal screws were in metaphyseal bone, they loosened and the construct did not provide rigid fixation as demonstrated in the x-ray (Figure 3) below that shows proximal screw loosening. Histology confirmed external callus formation and cortical translation with a visible

osteotomy gap. Therefore, in subsequent procedures the plate was placed more distally on the tibia to ensure that all four screws were placed in cortical bone.

Figure 3: Plain radiograph of pilot study at 5 weeks post fracture shows proximal screw loosening and callus formation

Furthermore, the integrity of the fibula may have impeded compression at the osteotomy site despite its contribution to stability. As previous research on fracture healing revealed that stress at failure in 3-point bending[117] and torsion[118] of healing tibial fractures were reduced in the absence of an intact fibula, the fibula integrity was preserved. Therefore, a narrower osteotomy had to be created, that could be compressed during plate fixation, and that remained in compression despite the effect of the intact fibula in preserving tibial length. Hence, a fine circular disc saw with a thickness of 0.1 mm (RS Components, UK, Kit no: 543-967) was used in conjunction with saline cooling. This circular disc saw was powered by a hand held Dremel® Multitool.

This modification in conjunction with a refined jig to accommodate the 0.1mm circular saw, achieved the desired compression at the osteotomy site in five cadaver tibia whilst the fibula integrity was preserved. This was then trialled in two rats.

However, between 1-2 weeks post fracture the tibiae had re-fractured through the most distal screw (Figure 4). It was considered that this was most likely related to stress concentration due to the relatively large screw diameter to bone size ratio[138].

Figure 4: Fracture through the 4th screw hole on the narrower area of the tibia distally when 1.4mm screws used.

Subsequently the screw diameter was reduced to 1.2mm. The plates were reduced in length and width, and the screw hole diameter reduced correspondingly. The plates were sized at 12mm x 3mm x 1mm. The dimensions for the screw holes on the jig had to be reduced accordingly. With these changes there were no further peri-prosthetic fractures. On plain radiographs, there was no evidence of external callus (Figure 5).

Figure 5: Radiograph 6 weeks post fixation with 12mm x 3mm x 1mm plate revealed no external callus

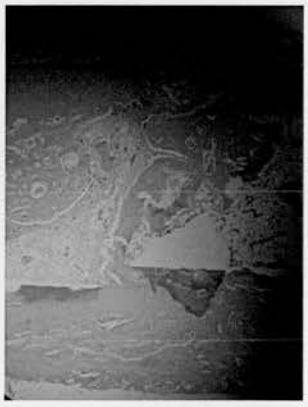

Figure 6: H&E stained coronal section at x5 magnification of tibia fixed with 1mm thick plate. Note cortical gap on upper surface. This area is opposite the surface of plate application

However, histological analysis of coronal sections revealed a small gap at the bone cortex on the far side away from the surface at which the plate was applied (Figure 6). In order to avoid this asymmetrical compression at the fracture site, the plates required pre-bending[139] to provide more even compression at the osteotomy during screw tightening. In order to permit pre-bending and plate conformation during screw tightening, the plate thickness had to be reduced whilst still maintaining an

adequate amount of stiffness. Trial plates of 0.8mm, 0.6mm and 0.4mm thickness were used to fix osteotomies in cadaver rat tibia. Taking into account the feasibility of manually bending the plate during surgery and the ability of the plate to conform to the tibial surface, a thickness of 0.4mm was chosen. The thicker plates were difficult to pre-bend and occasionally either displaced the fracture or cracked the bone during screw tightening when attempting to conform the plate to the tibial surface.

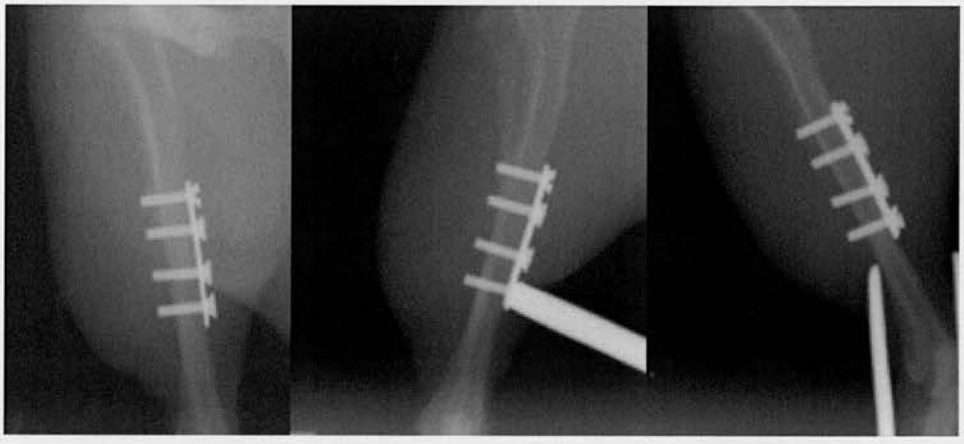

(a) (b) (c)

Figure 7: (a) A-P radiograph of plated tibia. (b) Valgus stress. (c)Varus stress. Note no widening or translation of osteotomy on stress application.

Subsequently the plate dimensions used for fixation of rat tibial osteotomies were 12 mm x 3 mm x 0.4 mm. Manual stress testing of this construct in 15 cadaver rat tibia revealed no macroscopic evidence of mobility at the fracture site on application of bending forces. This plate was then initially trialled in four animals. Immediate post operative Stress radiographs (Figure 7) did not reveal any opening of the osteotomy site. This produced healing with no visible callus on radiographs (Figure 8) and better symmetric compression across the fracture site (Figure 9). 'Contact-

healing' occurred at the cortical surface of plate application and 'gap-healing' was seen on the far cortex opposite to that of the plate. This finding was similar to that reported in the early studies of direct fracture healing that were performed in the rabbit[23], sheep[28] and dog[24,25]. Osteonal remodelling units, 'cutting-cones', were seen to traverse the fracture site (Figure 10, Figure 11).

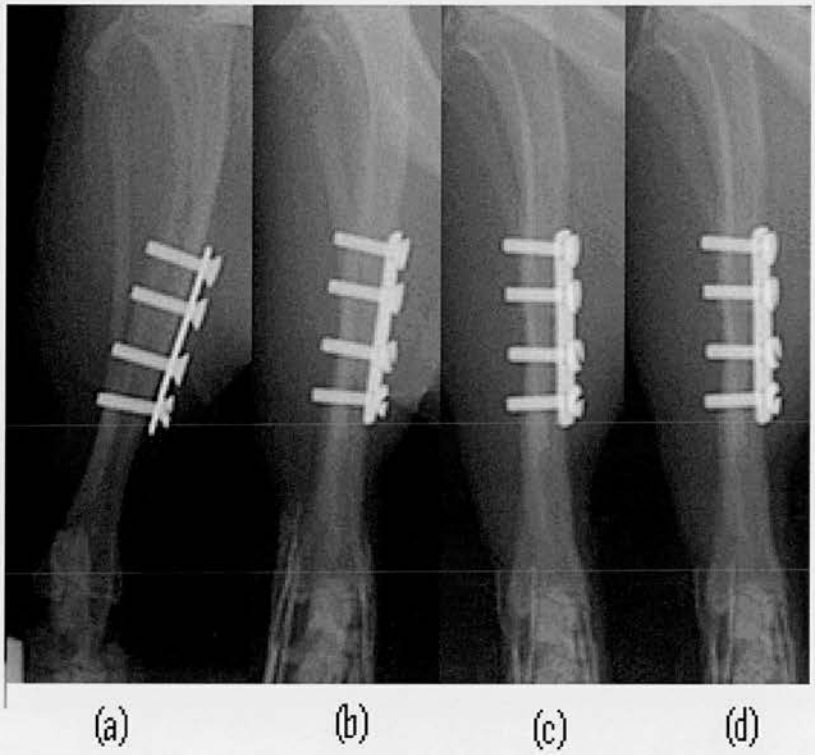

Figure 8: Plain radiographs following plate fixation (12mm x 3mm x 0.4mm) reveal no external callus, apposition of bone fragments and restoration of tibial alignment. (a) **Immediate post-op** (b) **2 wks post-op** (c) **4 wks post-op** (d) **6 wks post-op**

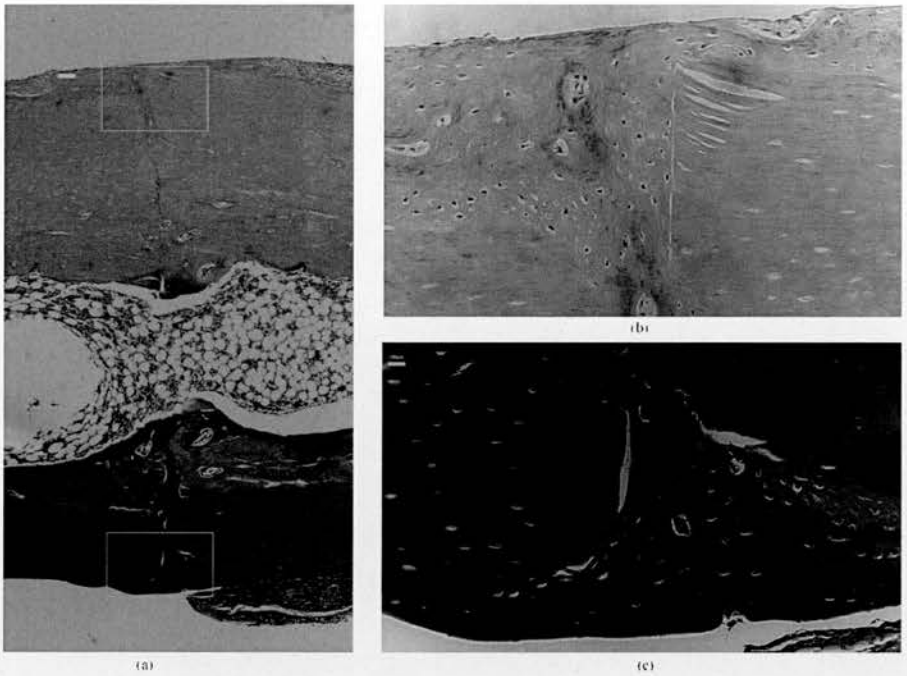

Figure 9: Masson's trichrome stain at 6 weeks post rigid compression plate fixation (a) x4 magnification shows osteotomy fragments aligned with no external callus. On the upper aspect note 'contact healing'on the cortical surface of plate application and 'gap healing' on the lower cortex opposite plate application. (b) x20 magnification 'contact healing. (c) x20 magnification 'gap healing' with deposition of new bone parallel to the line of osteotomy. Yellow line scale at 100µm

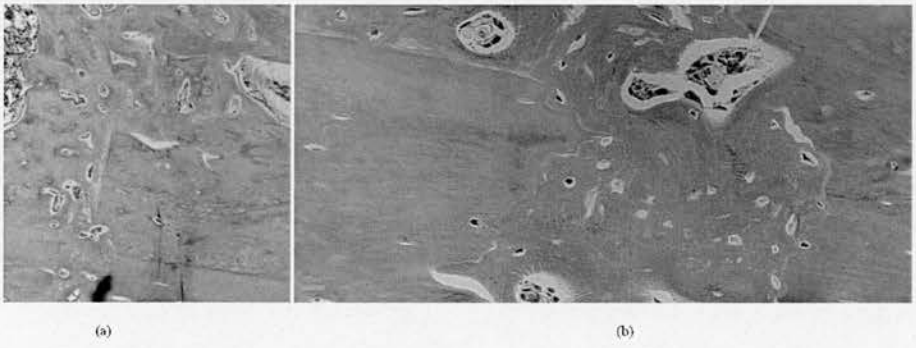

Figure 10: Masson's trichrome at 6 weeks post rigid compression plating (a) x4 magnification with 'cutting cone' (b) x20 magnification. Arrow shows osteonal remodelling unit traversing osteotomy site. Yellow scale line indicates 100µm

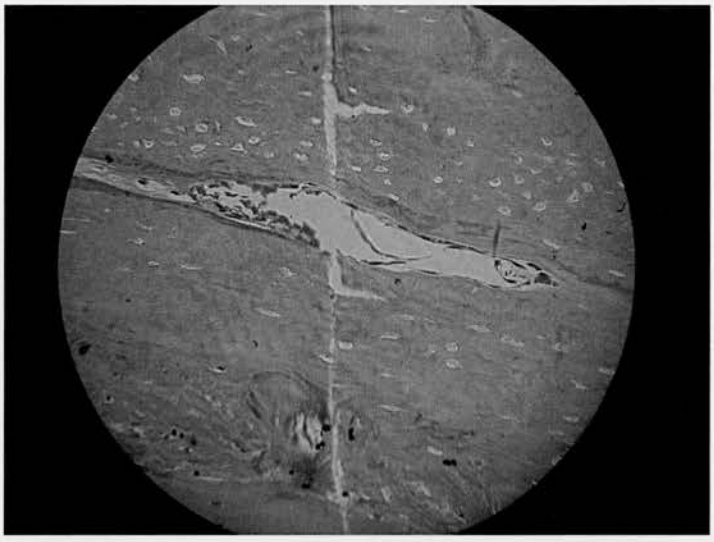

Figure 11: 'Cutting-cone' traversing osteotomy site in the rat model of direct fracture healing developed in this study. Note leading osteoclast on the right and new bone deposition behind the area of resorption.

The following table (Table 2) details the number of experimental animals and cadavers that were used at each stage of implant refinement for the development of this rodent model of direct fracture healing.

	Plate	Screws	Osteotomy	Cadaver n=	Animals n=	Observation
Initial Arrangement	16mm x 4mm x 1mm	1.6mmØ Proximal screws in metaphysis	0.5mm thick saw	10	2	Proximal screw loosening
1st Change	16mm x 4mm x 1mm	1.6mmØ All screws in diaphysis	0.1mm thick circular saw	5	2	Fracture at distal screws
2nd Change	12mm x 3mm x 1mm	1.2mmØ	0.1mm thick circular saw	5	4	Wide gap on far cortex
3rd Change	Pre-bent 12mm x 3mm x 0.8mm	1.2mmØ	0.1mm thick circular saw	5	0	Osteotomy displacement. Fracture on screw insertion
4th Change	Pre-bent 12mm x 3mm x 0.6mm	1.2mmØ	0.1mm thick circular saw	5	0	Osteotomy displacement. Fracture on screw insertion
Final Arrangement	Pre-bent 12mm x 3mm x 0.4mm	1.2mmØ	0.1mm thick circular saw	15	4	Better symmetric compression. Direct fracture healing.

Table 2: Implants used at each stage of refinement for development of the rat model of direct fracture healing.

Comparable Rat Model of Indirect Fracture Healing

The preservation of an adequate blood supply is crucial to fracture healing. The external fixator model[12] that had been previously used in our lab[140] involved significantly less soft tissue dissection than the plating model. Therefore a model of external fixation that used the same number and size of screw holes within the rat tibia to that employed in our plating model was developed.

This external fixator model was based on that of a uniaxial external fixator routinely used in clinical practice. Lengthier, 8 mm, M1.2 screws were used to secure the 12 mm x 3 mm x 0.4 mm plate, that performed the function of a uni-axial fixator, at a distance of 5 mm from the tibia. The plate was securely fixed to the screws with the aid of a cyanoacrylate adhesive (Loctite ®).

To permit comparison of bisphosphonate effects on these two fracture healing mechanisms the procedural aspects of the two fixation techniques were kept as similar as possible.

As in the rigid plating model the external fixators were initially trialled in ten cadaver tibia. On manual testing mobility was noted at the osteotomy site. When the external fixator was applied to four live rats initially they were observed to mobilise freely within 24-48 hours post surgery. External callus was seen on serial radiographs.

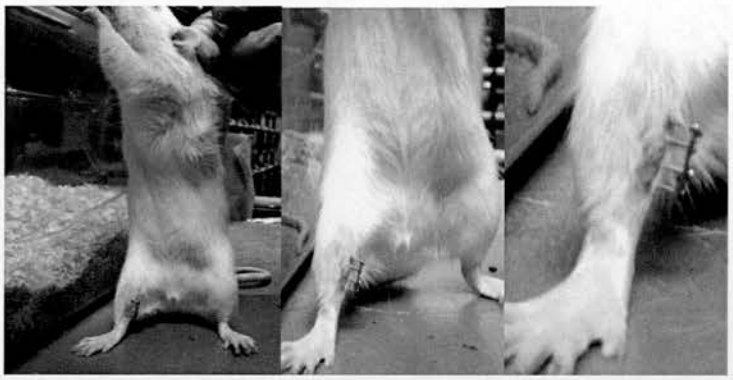

Figure 12: Unrestricted mobilisation post application of external fixator

Final Surgical Techniques Used Following Model Developments

Rigid Compression Plating of Rat Tibial Osteotomy

1. Animal weighed pre-operatively.
2. Inhaled Isofluorane for induction (5%) and maintenance (1-3%) of anaesthesia.
3. Pre-operative antibiotic prophylaxis administered, 1 mL/kg Synulox s.c (1ml Synulox contains 140mg Amoxicillin and 35mg Clavulinic Acid)

   This antibiotic treatment has been shown to significantly reduce bacterial counts in rat models of tibial staphylococcal osteomyelitis[141] when compared to other commonly used antibiotics.
4. Pre-operative fluids admistered, 10ml/kg 0.9% saline s.c.
5. Analgesia, 0.05mg/kg buprenorphine s.c.
6. Animal positioned supine. Right hind limb shaved, prepped with aqueous bethadine and a sterile drape applied.
7. 0.4mls/kg of 1% Xylocaine infiltrated into right hind leg prior to skin incision. This provides regional anaesthesia and vasoconstriction that aids visualisation of the operative field.
8. An antero-medial approach to the tibia exploiting the interval between *tibialis anterior* and *tibialis posterior*[142] used.

9. Then the custom made 4-hole jig (Physics Workshop, Edinburgh University, UK) (Figure 13) was applied to the flat medial surface of the tibia and secured to bone using two fine wires.

10. Four bone holes are drilled using a 1.0 mm drill bit powered with a hand-held Dremmel® Multitool under constant cool saline irrigation through the jig.

11. A fine circular saw of 0.1 mm thickness (RS Components, UK. Kit no: 543-967) used to create a transverse tibial osteotomy. The jig ensures compression at the osteotomy site during plate application.

12. The periosteum was stripped circumferentially from the tibia at the level of the osteotomy[23] for the length of one diameter of the bone width at the osteotomy site.

13. A pre-bent[139] 4-hole stainless steel plate (Physics Workshop, Edinburgh University, UK) measuring 12mm x 3mm x 0.4mm was applied to the medial surface of the tibia with four 1.2mm x 4mm stainless steel screws (PTS Ltd, East Grinstead, UK) to obtain rigid stability and compression across the osteotomy (Figure 15).

14. Following plate application the tibia was tested manually to assess mobility at the fracture site. The fixation was deemed inadequate if displacement was detected.

15. Wound closed with 3-0 vicryl.

16. Post-op Buprenorphine oral analgaesia (0.3mg/kg B.D) was administered in jelly cubes for 24 hours.

No restrictions to weight bearing were instituted. All animals were observed to be weight bearing within 24 hours post operation.

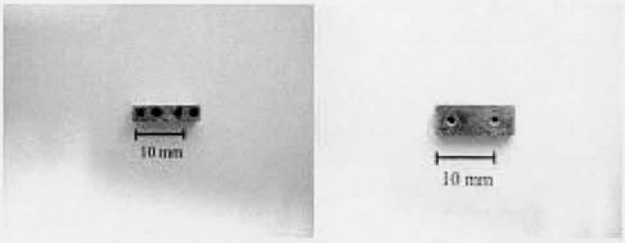

Figure 13: Custom made 4-hole jig. Two holes on lateral surface for threading of fine wire to help secure jig onto bone. Note there is also also a roughened surface to prevent the jig slipping on bone during drilling.

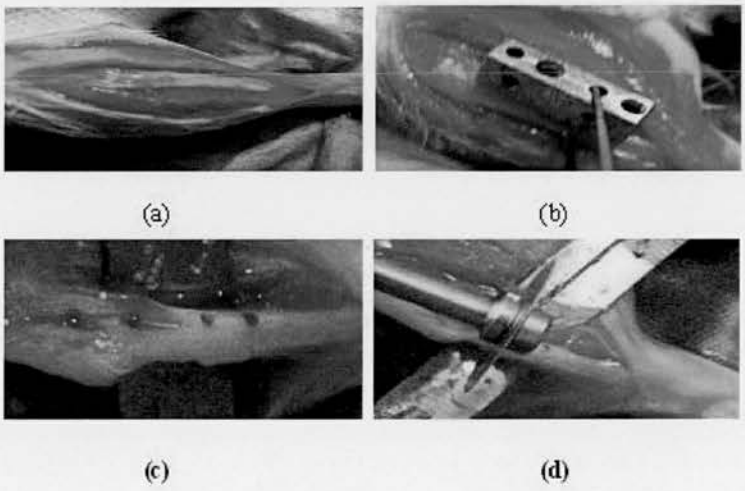

Figure 14: (a) Surgical approach (b) Custom jig (c) 4 drill holes on tibia (d) Osteotomy creation under saline irrigation.

Figure 15: Tibial plating showing anatomical alignment and compression at osteotomy site

External Fixation of Rat Tibial Osteotomy

Steps number 1 – 12 are performed as for rigid compression plating of a rat tibial osteotomy described earlier.

13. A four-hole stainless steel plate, of the same dimensions as that used for internal fixation, (Physics Workshop, Edinburgh University, UK) measuring 12 mm x 3 mm x 0.4 mm was placed at 5mm distance to the medial surface of the tibia with four M1.2 x 8 mm stainless steel screws of (PTS Ltd, East Grinstead, UK).
14. To prevent the plate from sliding on the screws Loctite® adhesive was applied to fix the plate to the screw heads.
15. Wound closed with interrupted 3-0 vicryl. The skin between each screw was approximated with a single stitch.
16. Post-op Buprenorphine oral analgaesia (0.3mg/kg B.D) was administered in jelly cubes for 24 hours.

Animals were permitted to weight bear without restriction (Figure 12) immediately post operatively.

Experimental Study on the Effects of Ibandronate on Fracture Healing

Animal Randomisation in to Experimental Groups

All animal procedures adhered to the Animals (Scientific Procedures) Act 1986 and were approved by the appropriate local and national authorities. Animals were fed standard rat chow and provided with water ad libitum. Animals were housed in individual cages at constant temperature (21 ± 1°C) and humidity (45% - 55%) using a 12 hour light/dark cycle. Following one week of housing to allow for acclimatisation to their new environment animals were randomly allocated to the experimental groups, as will be described later. Daily subcutaneous (s.c.) injections were then commenced for 3 weeks prior to operative fixation of a transverse tibial osteotomy. 6 weeks post surgical fixation animals were sacrificed (Figure 16). The mode of fracture fixation and daily injection varied according to the group that the animals were allocated to. All animals were weighed at weekly intervals.

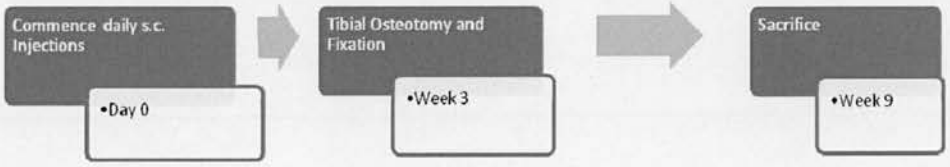

Figure 16: Timeline for animal surgery

Skeletally mature ex-breeder male rats aged between 11-13 months were used. A total of 36 animals were used. The optimal daily subcutaneous dose of Ibandronate to prevent bone loss in ovariectomised rats is 1μg/kg [143] and was therefore used in this study. The Ibandronate was purchased in pre-filled syringes from Roche as Bonviva®. Each syringe contained 3mg of Ibandronic acid in 3mL of solution (as

3.375mg of ibandronic acid, monosodium salt, monohydrate). The excipients within the solution are sodium chloride, glacial acetic acid, sodium acetate trihydrate and water for injection. The contents of each pre-filled syringe were diluted in isotonic saline to achieve the necessary concentration required for animal injection:

> 1mL Bonviva® (1mg/mL Ibandronic acid) diluted in 499mL isotonic saline
>
> , this produced; 1mg/mL Ibandronic acid in 500ml isotonic saline
>
> , this equals; 1µg Ibandronic acid in 0.5mL isotonic saline
>
> , therefore the daily volume of Ibandronate injection that each animal received was calculated as; 0.5mL x Animal Weight (in kilograms).

All animals were given a unique identification number. A card was created for each animal and all cards were mixed and placed in a box. Cards were randomly picked from this box and in this manner animals were randomly allocated to two groups of ten and two groups of eight. The two groups of ten were allocated to internal fixation (direct fracture healing). The two groups of eight were allocated to external fixation (indirect fracture healing). In both the direct and indirect fracture healing groups respectively, there was a placebo control group and a continuous bisphosphonate therapy group. For each group of animals half the number of animals were randomly allocated, similarly by picking numbered cards that were mixed in a box, for either mechanical testing or histological analysis of the healing tibial osteotomy following sacrifice.

The experimental groups are presented in Table 3.

		Direct, n=	Indirect, n=
Experiment 1 – Placebo Control	3 weeks of daily 0.5mL s.c injections of isotonic saline, osteotomy and stabilisation at day 21, then a further 3 weeks of daily s/c saline injections	10	8
Experiment 2 – Continuous Bisphosphonate Treatment	3 weeks of daily s/c 1µg/kg Ibandronate, osteotomy and stabilisation at day 21, then a further 3 weeks of daily s.c Ibandronate injections	10	8

Table 3: Experimental Groups

Sample Size Calculation

Restoration of function is the goal of fracture care. Stability at the healing tibial fracture site is the key element that permits weight bearing and is best assessed on mechanical testing. Mechanical testing also enabled direct comparison using identical methods between the two fracture healing mechanisms. Therefore, the primary outcome measure in this study was biomechanical testing.

The Act of Parliament governing the use of animals in scientific research states that a minimum number of animals consistent with a statistically significant result should be used (Home Office (HMSO) 1986). A sample size calculation was performed to ascertain the minimum number of animals required to detect a statistically significant difference. Sample size calculation was performed using MedCalc Software version 11.3.8 (Mariakerke, Belgium).

Based on results from a previous study[144] conducted within this research group using a rat tibial fracture model that revealed mean(±SD) following fracture healing in the control group as 150(±8.05)Nmm^{-2} a sample size of four per group was needed to detect a difference of 15% (20 Nmm^{-2}) in means using a two-sided, two-sample *t*-test with a 5% level of significance and an 80% power.

In order to ensure that there was a minimum of four animals for biomechanical testing and a further four for histological analysis at the end of the experimental period, ten animals were used in the plate fixation group and eight in the external fixation group. Due to the more complex procedural aspects of internal fixation it was anticipated that there may be a greater likelihood of failure therefore additional

animals were used to ensure that there would be an adequate number of animals that proceeded successfully through to the end of the experimental process for meaningful analysis of results.

Mechanical Testing

The mechanical properties of the healing tibial osteotomies were assessed using four-point bending.

Testing Apparatus

Mechanical testing was performed using a custom made jig (Figure 17) previously designed by University of Edinburgh Physics Workshop, Kings Buildings, Edinburgh for testing rat tibiae in four-point bending[144] in conjunction with a Zwick/Roell Z005 materials testing machine. The upper rig was designed to incorporate a pivot to ensure an equal application of force at all 4 loading points[113] during the bending tests of rat tibiae, which were irregularly shaped. The upper loading span was spaced 10 mm apart and the lower static span was spaced 20 mm apart. Contact points were rounded to minimise notching of the bone after load application.

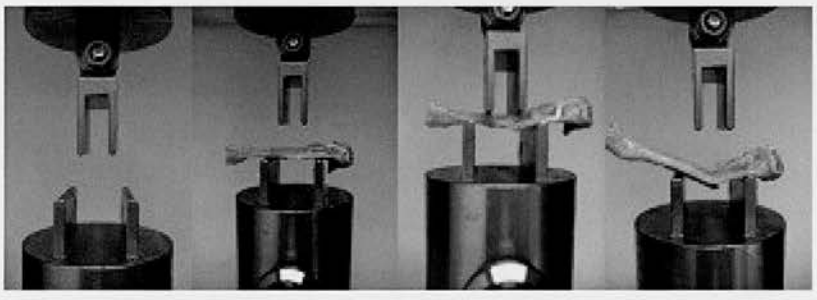

Figure 17: Mechanical testing jig and sequence of 4-point bending test

The Zwick/Roell Z005 material testing machine had a load cell of 10 kN and load was applied at a rate of 10 Ns^{-1}. A stiff load cell in relation to bone was used to

eliminate deformation in the testing apparatus. Therefore, the deformation noted would be primarily within the bone tested.

Specimen Storage

Following sacrifice of animals at six weeks post osteotomy, tibiae were collected after careful dissection of soft tissues then stored in 0.9% Saline and frozen at -20°C, prior to performing mechanical tests within three weeks.

Specimen Preparation

Specimens in frozen saline were warmed within individual tubes in a water bath set at 37°C for at least 30 minutes prior to mounting on the testing apparatus for four-point bending.

Specimen Testing

Tibiae were mounted horizontally with the lateral surface resting on the lower rig. This position was adopted as the tibiae were found to be stable on the testing apparatus in this orientation. The vertical distance from the medial tibial plateau to the healing osteotomy was measured with calipers and recorded. The site of the healing osteotomy was positioned to lie in the middle of the two lower loading points. In the contra-lateral tibia, a site corresponding to the vertical distance of the healing osteotomy from the medial tibial plateau was marked with a pencil. Similarly, this site was positioned in the middle of the two lower loading points.

All specimens were tested to failure. A load-deflection curve was obtained for each specimen during mechanical testing. A typical load-deflection curve that was

obtained for a healing osteotomy (Chart 2) and intact tibia (Chart 3) are shown below. Note that for the healing osteotomy that there was no distinct yield point indicating that specimen failure occurred at the point of ultimate load that was not distinguishable from the yield point. In the intact tibia the yield point was noted to be distinct from the ultimate load at failure.

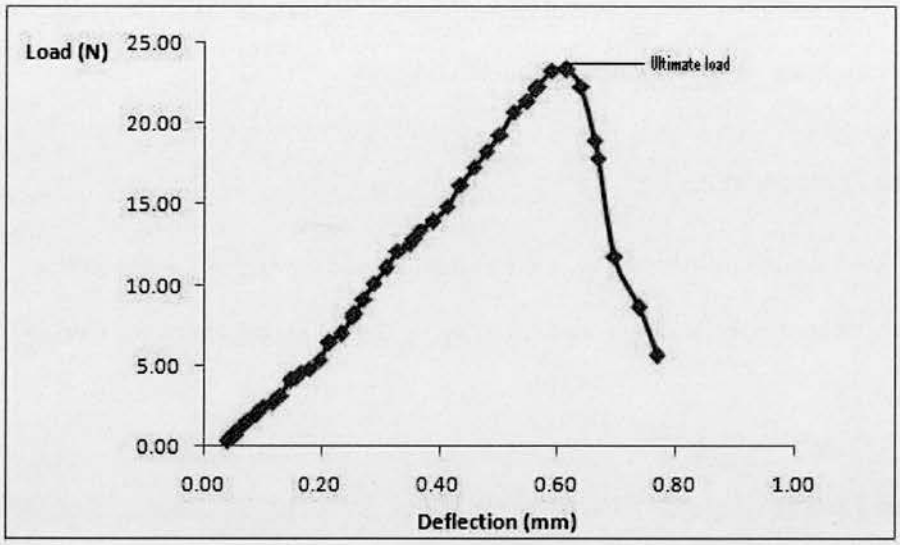

Chart 2: Typical load-deflection curve obtained for a healing tibial osteotomy. Note no distinct yield point that is separate to point of ultimate load.

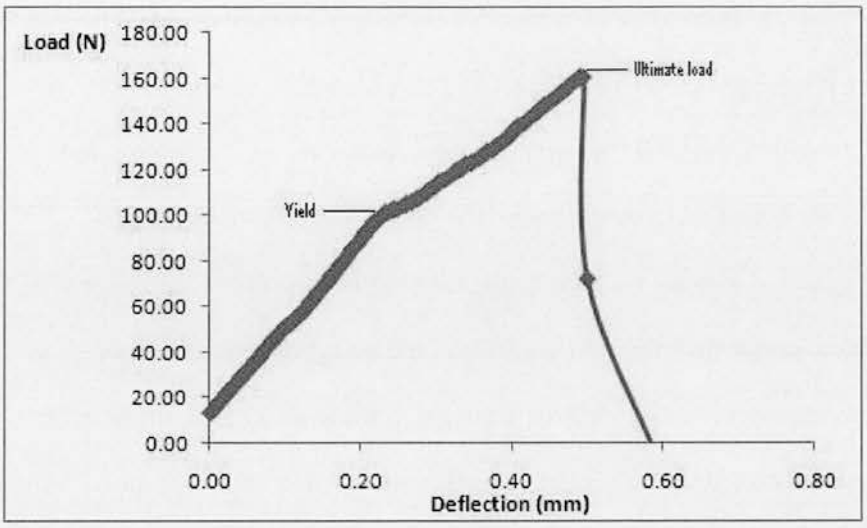

Chart 3: Typical load-deflection curve obtained for intact tibia.

Work-to-Failure

In the intact tibia, the area under the load-deformation curve was measured to quantify work to failure. This represents the amount of energy required to create a fracture in the bone.

Physical Measurements of Bone following Mechanical Test to Failure

Digital images obtained following preliminary bending test on cadaveric tibiae kindly donated by the Biological Research Facility (BRF), The University of Edinburgh revealed that the cross section of the rat mid-tibial shaft most closely resembled a triangle (Figure 18).

Measurements were made of the distal segment of bone after mechanical testing to failure. The sagittal and coronal widths which corresponded to the external vertical height (*H*) and external base length (*B*) of the triangular cross section (Figure 18) were obtained using sliding callipers. A digital image (Canon Digital IXUS 75

camera) of the distal segment cross section for each sample was obtained. These images were printed and the vertical height and base length of the triangular cross section for the whole bone and the intramedullary canal were measured manually. The scale for the digital image was obtained by comparing the external widths previously measured with the callipers to the readings obtained from the image. The internal vertical height (h) and base length (b) of the triangular intramedullary cross section were then calculated. The triangular cross sectional area of the whole bone and intramedullary canal were then derived. This was used to obtain the cross sectional moment of inertia(I) that was required to calculate the stress(σ), according to the elastic beam bending theory.

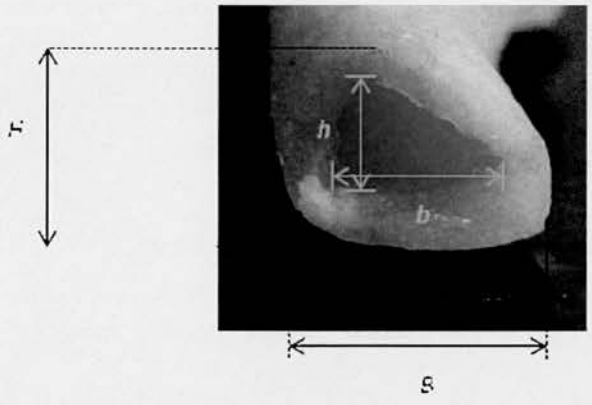

Figure 18: Cross section of tibia. H = external vertical height, B= external base length, h= inner vertical height, b= inner base length

Cross Sectional Moment of Inertia

The maximum stress at failure for the bone in bending test was related to its material properties and its physical shape. Bending caused predominantly tensile forces at the convexity and compression within the concavity in the plane of bending.

These forces were greatest at the bone surface and absent at the centre of mass (the neutral axis). The cross-sectional moment of inertia (I) is a property of a shape that is used to predict its resistance to bending and deflection based on the distribution of the shape surrounding the neutral axis in bending[113]. I is required to calculate stress. The cross section of the mid tibial shaft most closely resembles a triangle (Figure 18). Therefore the cross-sectional moment of inertia was calculated for a triangular cross section using the following formula[145]:

$$I = \frac{(B \times H^3) - (b \times h^3)}{36}$$

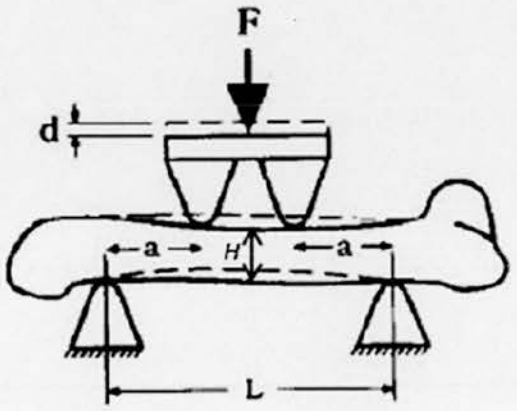

Figure 19: Diagram of 4-point bending with explanation of abbreviations used in equations to calculate stress, and theoretical strain.

F = Applied force
a = Distance between the inner and outer loading points = 5mm
H = Vertical height of triangular cross section
L= Distance between outer loading points =10mm
d = Displacement

Stress

Stress is defined as the force applied per unit area. The elastic beam bending theory states that Stress (σ) is derived from the following formula[145]:

$$\text{Stress, } \sigma = \frac{M \times Y}{I}$$

Where,

$$\text{The applied moment, } M = \frac{F}{2} \times a$$

The applied force is halved as it is distributed between two points of load application

$$\text{The distance from the neutral axis, } Y = \frac{h}{3}$$

For a triangular cross-section, the neutral axis is 1/3 of the way between the base and the vertical height to the apex of the triangle.

Therefore, the equation used in this particular experiment to calculate stress was:

$$\sigma = \frac{\left(\frac{F}{2} \times a\right) \times \frac{h}{3}}{I}$$

$$= \frac{F \times a \times h}{2 \times 3 \times I}$$

$$= \frac{Fah}{6I}$$

During bending tests it was observed that specimens failed in tension (Figure 17).

In addition to the assumption that rat tibiae have a triangular cross section at the mid-shaft, the following standard assumptions for the elastic beam bending theory were used[122]:

1. The span did not change during the test
2. No horizontal stresses developed at the supports
3. No stress concentrations developed at the contacts
4. The slope of the neutral axis was small at all points compared to unity
5. The strain of any "fibre" was proportional to its distance from the neutral axis
6. Shearing stresses were negligible
7. The loads were in one plane and perpendicular to the neutral surface
8. The beam was narrow.

The stress at failure as a surrogate of absolute bone strength was calculated and recorded for each specimen.

Theoretical Strain

Strain is defined as the proportion change in length or relative deformation. Theoretical strain (ε) was calculated using the following equation for 4-point loading[113]:

$$\text{Strain}, \varepsilon = \frac{6Yd}{a(3l - 4a)}$$

Toughness

Following calculation of stress and theoretical strain a stress-strain curve was produced for the intact tibia. The area under the curve to the point of ultimate stress was used to quantify toughness (u)[146]. This represents the quantity of energy absorbed per unit of bone prior to failure.

Radiography

Serial Radiographs of Healing Osteotomies

In order to assess the progression of fracture healing serial plain radiographs were obtained for all animals. Plain radiographs were taken immediately post-operatively, thereafter at two, four, and six weeks post-operatively. Plain radiographs were obtained using a portable X-ray unit (Acu-Ray JR, Stern Manufacturing Toronto, Canada) with an output of 60 kV and exposure time of 0.1ms. Images were captured on digital x-ray plates (Fuji IP Cassette, Fuji Photo Film Co Ltd Japan).

Standardised antero-posterior (A-P) radiographs were obtained. Under general anaesthesia the animals were placed supine on the x-ray plates. The hip and knee were flexed to 90° and the ankle was grasped with a padded retort stand (Figure 20). The x-ray beam was positioned at a fixed distance, 78cm from the plate.

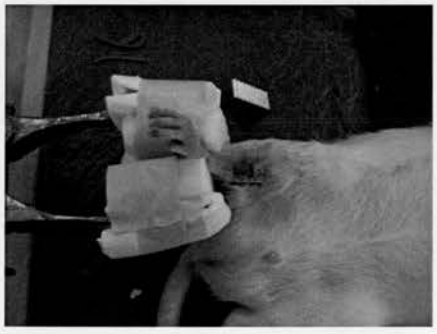

Figure 20: Rat positioning to obtain standardised antero-posterior radiograph of tibia

Serial radiographs were qualitatively assessed looking in particular for maintenance of alignment, appearance of callus, visibility of osteotomy and for any evidence of implant loosening.

Callus Index

In the external fixator groups the callus index was measured in serial radiographs at two, four and six weeks post osteotomy to assess the progression of fracture healing. Using Image-J software (National Institutes of Health, USA) the maximum callus diameter (c) and bone diameter (b) were measured (Figure 21) in pixel units. The callus index was calculated as follows:

$$\text{Callus index} = \frac{c}{b}$$

Where, c = Maximum diameter of callus.

b = Diameter of diaphyseal bone at similar level to callus.

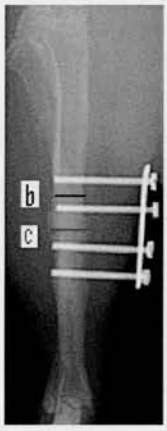

Figure 21: A diagram of the method used to determine callus index

Radiographs of Extricated Tibiae

Following sacrifice at six weeks post osteotomy, tibiae were carefully dissected of soft tissue and metalwork removed. Plain radiographs were obtained using a portable x-ray unit (Acu-Ray JR, Stern Manufacturing Toronto, Canada) with an output of 60 kV and exposure time of 0.1ms. Images were captured on digital x-ray plates (Fuji IP Cassette, Fuji Photo Film Co Ltd Japan). The x-ray beam was placed at a fixed

distance of 78 cm from the x-ray plate. The bones and an aluminium step-wedge consisting of ten, 1mm steps, were placed on the x-ray plate for image capture. Lateral radiographs of both tibiae in each animal were obtained to exclude the effect of fibula overlay. The aluminium step wedge was used to peform radiographic analysis of bone density as will be described later

Visibility of Osteotomy Site

The visibility of the healing osteotomy sites were scored as absent (0), partially visible (1) or totally visible (2) as previously described[61,130] (Figure 22). The radiographs were scored by two assessors on two separate occasions independently. The radiographs were randomised and the assessors were blinded to the fixation method and bisphosphonate dosing regimen. One of the assessors was the author and the other an orthopaedic trainee who did not have any other involvement in this study.

Figure 22: X-rays of extricated tibiae demonstrating scoring for visibility of osteotomy

Callus Width

The maximum sagittal callus diameter (Figure 23) was measured from a contact lateral radiograph of the extricated tibiae from the external fixation groups following sacrifice at six weeks post osteotomy. The maximum coronal callus width was measured from the A-P radiograph at 6 weeks post-osteotomy as described previously in the section on callus index (Figure 21).

Figure 23: A diagram of method used to measure sagittal callus width

Radiographic Analysis of Bone Density

An aluminium step-wedge (Figure 24) consisting of ten, 1mm steps was placed near the area of interest in each intact limb x-ray. Image analysis was performed in MATLAB® (The MathWorks, Inc. MA, USA). Each radiograph was corrected for background variation due to the Anode-Cathode Heel effect by the fitting and subtraction of an exponential model to the intensity profile in a blank area of the image. A calibration graph of Aluminium step thickness (mmAl) versus the grey level in each step of the step wedge was then made. This was fitted with an exponential curve and provided a calibration between measured grey level and Aluminium equivalent (Al.Eq) density for any point on the radiograph[147].

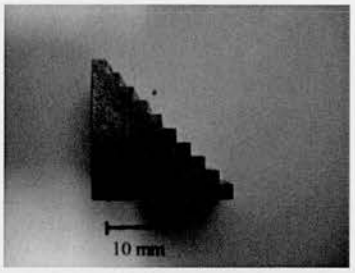

Figure 24: Aluminium step wedge with ten, 1mm steps

In the uninjured contra-lateral limb of the continuous bisphosphonate treatment and placebo groups the point where the fibula joined the tibia distally was marked. A 100 x 50 pixel box was marked from this point to include the mid-shaft of the bone. To assess bone density, an average grey level of the diaphyseal tibia within this box was measured. This measured grey level was then converted to an Aluminium Equivalent (Al.Eq) density as previously described.

Histology

This was performed to assess morphology at the fracture site. In order to obtain sections with optimum preservation of cellular architecture samples were fixed in formalin, decalcified and embedded in paraffin.

Fixation

At 6 weeks post-osteotomy, following sacrifice the tibiae and fibulae from each animal were dissected out. Within 30 minutes of extrication, the specimens were immersed in 10% formalin in phosphate buffered saline at pH 7.2-7.4 for 48 hours.

Decalcification

Based on a previous experiment[144] all specimens were decalcified for 4 weeks in EDTA at pH 7 and 37°C with weekly changes of EDTA. Complete decalcification of initial specimens were verified using a table top x-ray unit (Faxitron, USA)

Processing

Following decalcification an automated processor was used to prepare specimens for embedding in paraffin. The processing protocol is shown in Appendix 1. The specimens were mounted in paraffin blocks and orientated vertically to permit longitudinal cross sections of the tibia to be made in the coronal plane.

Sectioning

5μm sections were cut on a standard microtome (Shandon). After floating on deionised water at 40°C to remove ridges, sections were mounted on 'Superfrost plus' slides (BDH). Slides were stood vertically to dry and then baked at 37°C for 12 hours to increase section adherence. All slides were then stored in a dry, dark environment at room temperature until used in histological procedures.

Analysis of Sections

For this study coronal sections of the tibia were chosen as this allowed visualization of the cortical surface of plate application and the opposite far cortex with the intervening intramedullary space in a single view. This permitted examination for the presence of external callus, contact healing on the plate surface and gap healing on the far cortex.

In order to study the general morphology of the healing fractures a series of coronal sections were made at three sites. To avoid sections that were solely within the anterior cortex, the first site was 100μm from the anterior cortex. After leaving a space of 500μm the second series of sections were made and finally the third series of sections was similarly spaced 500μm apart. Each site was spaced 500μm apart to assess variability within the specimen. Serial 5μm coronal sections were made at each point to permit the use of 2 staining techniques (H&E and Masson's Trichrome). All slides were assessed in a blinded manner following randomisation.

On completion of the first series of experiments with rigid plate fixation where animals either received placebo or continuous bisphosphonate therapy a random sample of twenty slides, one-third of specimens, from these animals were presented

to a musculoskeletal pathologist who had not been involved in the experimental study design and execution to assess the general morphology at the fracture site. This was to ensure that an independent assessor evaluated the specimens qualitatively in an unbiased manner.

Similarly in a blinded and randomised manner all slides were assessed by the author and the pre-dominant tissue type at the fracture site was evaluated and reported as cartilage(1), undifferentiated mesenchymal tissue(2), or bone(3). The mode of the tissue type that was predominant amongst the slides for each animal was used in subsequent analysis. Furthermore, the presence or absence of new bone formation immediately across the osteotomy site was noted.

Results

Animal Outcomes

All animals were fully weight bearing within 12 hours post-operatively. Animal weights remained relatively unchanged during the 6 week period post fracture stabilisation prior to sacrifice.

Exclusions

One animal in the control ex-fix group (SX05) developed a wound infection in the first week post operatively. This animal was treated with daily subcutaneous injections of antibiotics (Synulox) and within four days there were no visible signs of infection. When the external fixator was removed, on animal sacrifice, there was gross mobility at the fracture site. Therefore this animal was excluded from subsequent data analysis. In another animal in the control ex-fix group (SX06), the fixation failed at two weeks post op with marked angulation and displacement at the fracture site. Due to fixation failure, no subsequent analysis was performed for the injured limb in this animal.

In the plate fixation group an animal in the control group (S01) had an abnormally high force at failure of the healing osteotomy. On close inspection of the serial radiographs and lateral contact radiographs, the posterior cortical hinge was intact suggesting that the osteotomy was not completed posteriorly. External callus was observed on the posterior cortex of one animal in the bisphosphonate plating group (C02) on contact radiograph following sacrifice and plate removal. This was likely to have occurred due to inadequate stripping of the periosteum on the posterior surface of the tibia where there is a broad and more extensive attachment from the deep

muscles of the posterior compartment. Data from these two animals were excluded from subsequent analysis.

Injured Limb

Following sacrifice, at 6 weeks post osteotomy and stabilisation, tibiae were extricated. After careful dissection of soft tissues, the metalwork was removed in the injured limbs. A standardised contact lateral radiograph was obtained, then specimens were either tested to failure with four-point loading or processed for histological analysis as per randomisation at the onset of the experimental procedure.

Mechanical Testing

In the direct healing group, mechanical testing data was available for analysis from four animals respectively in the control and bisphosphonate treatment groups. Two-sided, two sample *t*-tests were used for comparison of the mean values between each of the two groups. The control plate group had a statistically significant, $p = 0.017$, higher mean (±SD) stress at failure 24.65 (±6.15) Nmm^{-2} compared to the bisphosphonate treated plate fixation group 8.69 (±7.63) Nmm^{-2}.

In the indirect fracture healing group, the mean (±SD) stress at failure for the four animals where mechanical testing was performed in the bisphosphonate treated external fixation group was 28.70 (±16.15) Nmm^{-2}. Due to infection and fixation failure, there were only two animals in the control external fixation group where mechanical testing data was available. The stress at failure in these two animals SX02 and SX07 respectively were 23.94 Nmm^{-2} and 19.71 Nmm^{-2}. There was a trend towards a greater stress at failure for the bisphosphonate external fixation group compared to the bisphosphonate plating group, $p = 0.066$. The stress at failure was similar between the bisphosphonate ex-fix and control plating groups. The

distribution of the stress at failure values for the healing tibial osteotomies are presented in Chart 4. All mechanical testing measurements are listed in Appendix 2

.

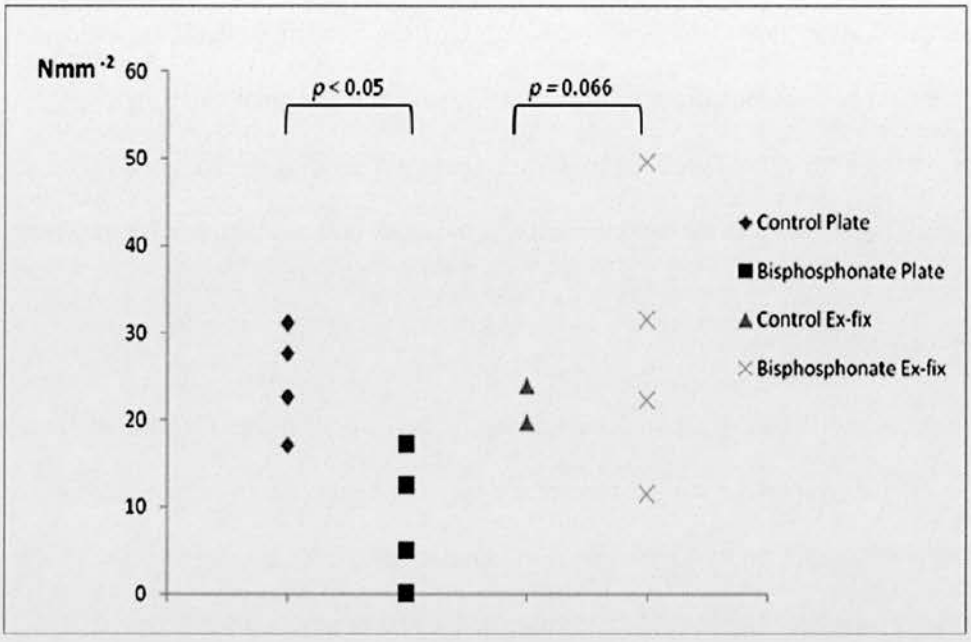

Chart 4: Distribution of stress at failure values for healing tibial osteotomies

Radiography

Serial Radiographs of Healing Osteotomies

Serial antero-posterior (A-P) radiographs of healing osteotomies in the control and bisphosphonate plating groups revealed no evidence of external callus formation (Figure 25). One animal in the bisphosphonate plate group had callus on contact radiographs following sacrifice and plate removal. This animal was excluded from analysis as previously described in the section on 'Exclusions' above.

In the external fixation groups the A-P radiographs revealed external callus formation (Figure 26). In one animal in the control external fixator group that developed an infection (SX05) there was marked resorptive changes on the serial A-P radiographs from the second post-operative week onwards. In the other animal within the control external fixator group that was excluded from subsequent analysis (SX06), there was marked angulation and displacement at the fracture site from the second post-operative week onwards.

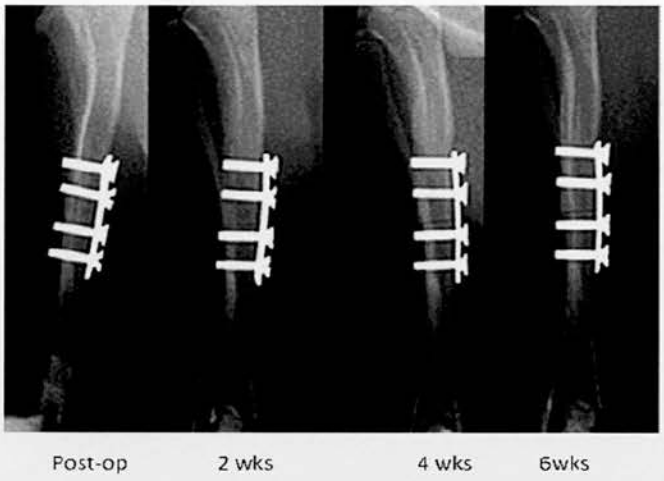

Figure 25: Serial x-rays of a bisphosphonate treated animal with rigid plate fixation. Note no external callus formation and anatomical reduction, but persistence of fracture line.

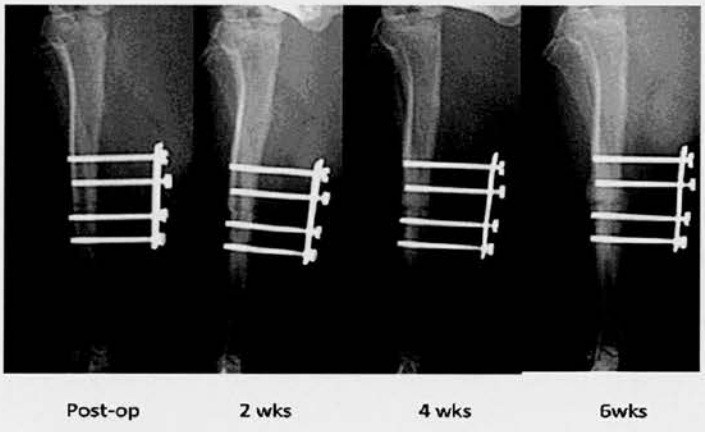

Figure 26: Serial x-rays of an animal with external fixator stabilisation of tibial osteotomy. Note external callus formation.

Callus Index

The callus index was measured at 2, 4 and 6 weeks for animals in the external fixator groups. The callus index in the control animals (Chart 5) that received saline injections appeared to peak at week 4, then declined at the 6 week stage. In contrast the callus index of osteotomies stabilised with an external fixator in animals that received ibandronate continued to rise up to 6 weeks (Chart 6).

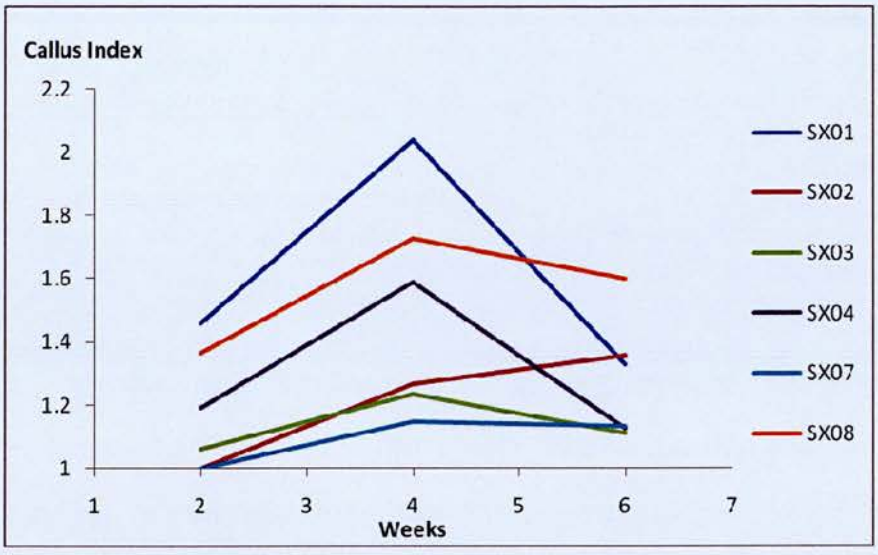

Chart 5: Serial measurements of callus index in the control external fixator group indicating a peak in callus index at between 4 to 6 weeks post osteotomy.

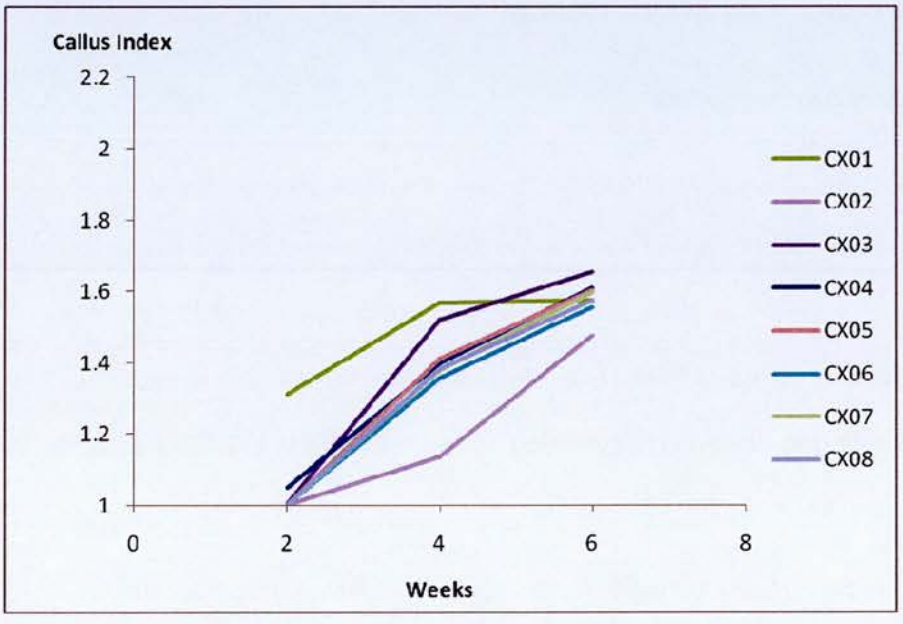

Chart 6: Serial measurements of callus index in the ibandronate external fixator group indicating callus index continues to rise after 4 weeks.

Callus Width

Radiographic measurements of the callus width were made for the external fixator groups. Coronal width was measured from the antero-posterior x-ray at 6 weeks. Sagittal width was measured from the lateral x-ray following sacrifice and implant removal.

The mean(±SD) for the coronal and sagittal callus width in the control external fixator group was respectively 4.49(±0.78) pixel units and 4.62(±1.04) pixel units. For the ibandronate external fixator group the mean(±SD) coronal and sagittal widths were 5.04±(0.67) pixel units and 5.17(±1.27) pixel units. A two-sided, two sample *t*-test revealed no statistically significant difference in these measurements between the two groups.

The callus index and callus width measurements are listed in Appendix 3.

Visibility of Osteotomy Site

The Kappa values were used to assess for inter and intra rater agreement for osteotomy line visibility There was good inter-rater agreement for the assessment of fracture line visibility between the two observers with a κ value of 0.77 (95% confidence interval (CI) 0.59 to 0.94). Similarly, there was good intra-rater agreement for both observers [Author (κ=0.87, 95% CI 0.74 to 1.00), Independent assessor (κ=0.64, 95% CI 0.43 to 0.86).

Contact radiographs following 6 weeks of fracture healing showed that the osteotomy line remained more clearly visible in the bisphosphonate plate group compared to the control plate group. The score, 'absent' (0), was not used by either observer for the bisphosphonate plate group animals but used to describe 4 to 6 of 9

animals in the control plate group on each occasion (Table 4). Chi square tests showed that this difference was statistically significant ($p < 0.01$).

Comparison of osteotomy line visibility in the indirect fracture healing groups revealed no difference between animals treated with bisphosphonate and controls that received saline injections (Table 5). All scores for the visibility of the osteotomy line are presented in Appendix 4.

		Plate Fixation Group	**Absent**	**Partially Visible**	**Totally Visible**	**Chi squared test *p*-value**
Author	1st assessment	Bisphosphonate	0	4	5	<0.005
		Control	5	4	0	
	2nd assessment	Bisphosphonate	0	4	5	0.006
		Control	4	5	0	
Independent assessor	1st assessment	Bisphosphonate	0	3	6	<0.005
		Control	5	4	0	
	2nd assessment	Bisphosphonate	0	5	4	<0.005
		Control	6	3	0	

Table 4: Number of animals in each group based on the visibility of the osteotomy site as scored by two observers on two separate occasions for animals treated with plate fixation.

		External Fixation Group	Absent	Partially Visible	Totally Visible	Chi squared test *p*-value
Author	1st assessment	Bisphosphonate	0	5	3	0.687
		Control	0	4	2	
	2nd assessment	Bisphosphonate	0	4	4	0.589
		Control	0	3	3	
Independent assessor	1st assessment	Bisphosphonate	1	3	4	0.459
		Control	0	4	2	
	2nd assessment	Bisphosphonate	0	4	4	0.469
		Control	0	5	1	

Table 5: Number of animals in each group based on the visibility of the osteotomy site as scored by two observers on two separate occasions for animals treated with external fixation.

Histology

Based on the general appearance at the fracture site an independent assessor (a fully qualified musculoskeletal pathologist) when viewing a sample of slides from the two plating groups (placebo control and continuous bisphosphonate treatment groups), in a blinded fashion, was able to allocate all slides into two distinct groups. All slides within the first group, where there was less fracture repair activity, were from bisphosphonate treated animals. The other group of slides consisted wholly of specimens from controls. There were no slides that were not clearly distinguishable between the groups (Figure 27)

The predominant tissue type was bone in all five control plate fixation animals. In the bisphosphonate plating group, three animals had predominantly cartilage like tissue at the fracture site and the remaining two assessed had predominantly undifferentiated mesenchymal tissue. A chi-squared test revealed a p-value of 0.007 indicating a significant difference in the predominant tissue type at the osteotomy site between the bisphosphonate plate and control plate groups. In only two of five animals in the bisphosphonate treated plating group was there histological evidence of new bone formation across the osteotomy.

In the indirect fracture healing groups, the predominant tissue type across the osteotomy site in all animals was undifferentiated mesenchymal tissue. There was new woven bone formation within the callus of all animals treated with external fixation, both in the control and in the bisphosphonate treated animals (Figure 28)

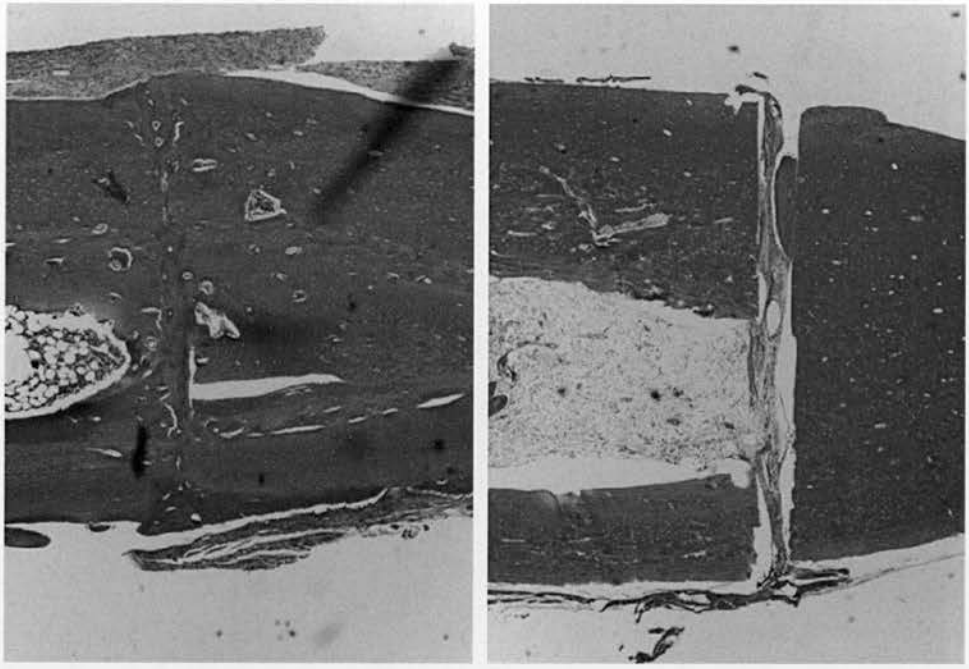

(a) (b)

Figure 27: Masson's Trichrome (x4) magnification. (a) Control plate fixation. Note primary healing with bone formation. (b) Bisphosphonate plate fixation. Note little activity at the fracture site with cartilage formation. Yellow line scale at 100µm.

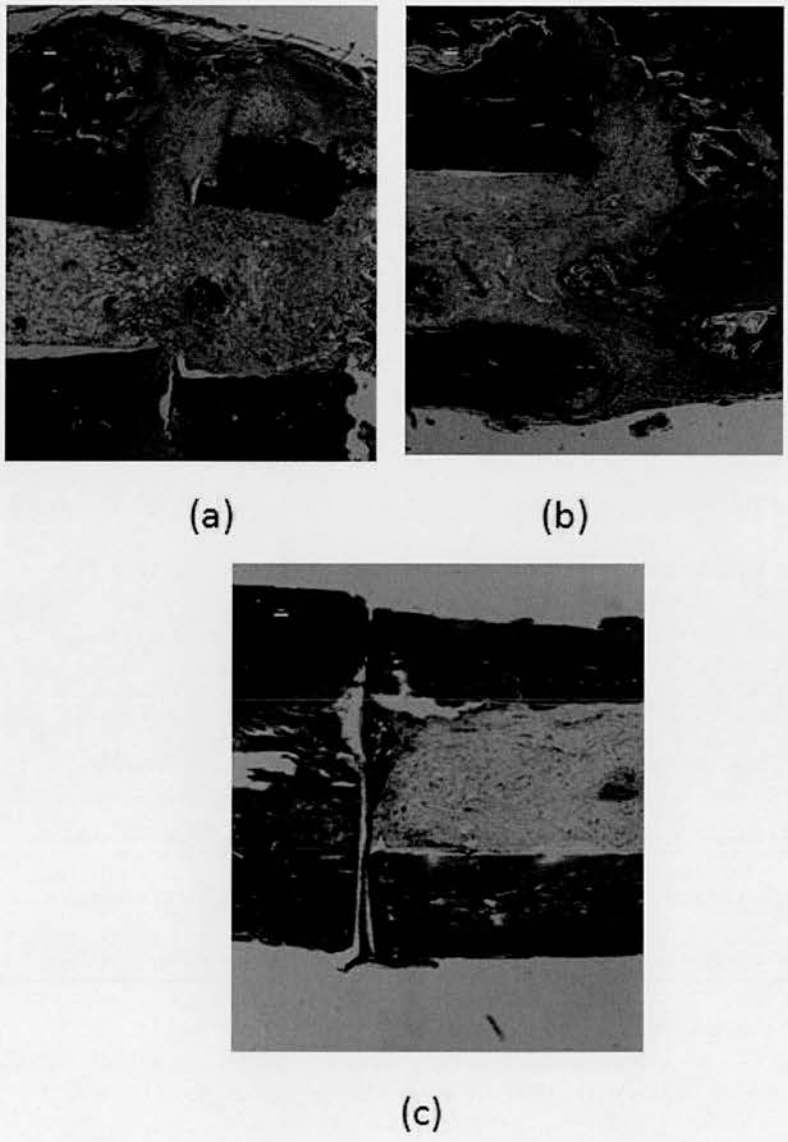

Figure 28: Masson's Trichrome (x4) magnification. (a) Control external fixation. Note woven bone formation within external callus. (b) Bisphosphonate external fixation with rim of external callus and new woven bone formation, in contrast to (c) Bisphosphonate plate fixation with little activity at the fracture site and no new bone formation. Yellow line scale at 100μm.

Uninjured Limb

Mechanical Testing

Mechanical testing data was available for the uninjured tibia for 14 animals that received daily bisphosphonate therapy and for 17 animals that received placebo saline treatment. Two animals in the bisphosphonate group (CX07 and CX08) were excluded from analysis, as failure of the intact tibia occurred in a mode not consistent with bending stress.

Two-sided, two sample *t*-tests were used to assess for differences between the mean values of mechanical parameters that were analysed between the two groups. The bisphosphonate group had a statistically significant, p=0.006, higher mean (±S.D) stress at failure 219.2 (±45.99) Nmm^{-2} compared to the placebo group 169.5 (±43.32) Nmm^{-2} (Chart 7). There was no significant difference in toughness between the bisphosphonate treated group in comparison to placebo controls [Bisphosphonate v. Placebo = 2.51(±1.74) $MJmm^{-3}$ v. 1.67(±0.86) MJ/mm^{-3}]. Similarly there was a greater, but not statistically significant, mean work-to-failure in the bisphosphonate group compared to placebo controls [76.37 (±50.74) J v. 52.94 (±23.94) J]. The deflection to the point of failure was greater in the bisphosphonate group but not significantly different [Bisphosphonate v. Placebo = 0.68(±0.23) mm v. 0.55(±0.27) mm].

There was no statistically significant difference in the physical measurements of bone width (two-sided, two sample *t*-test). The mean (±SD) coronal bone widths for the bisphosphonate v. placebo control groups respectively were 3.7 (±0.83) mm v. 3.8 (±0.62) mm and the mean sagittal bone widths were 2.7 (±0.24) mm v.

3.0(±0.21)mm. There was no difference in the cross sectional moment of inertia between the groups [Bisphosphonate v. Placebo = 0.97 (±0.07) mm^4 v. 1.01 (±0.08) mm^4].

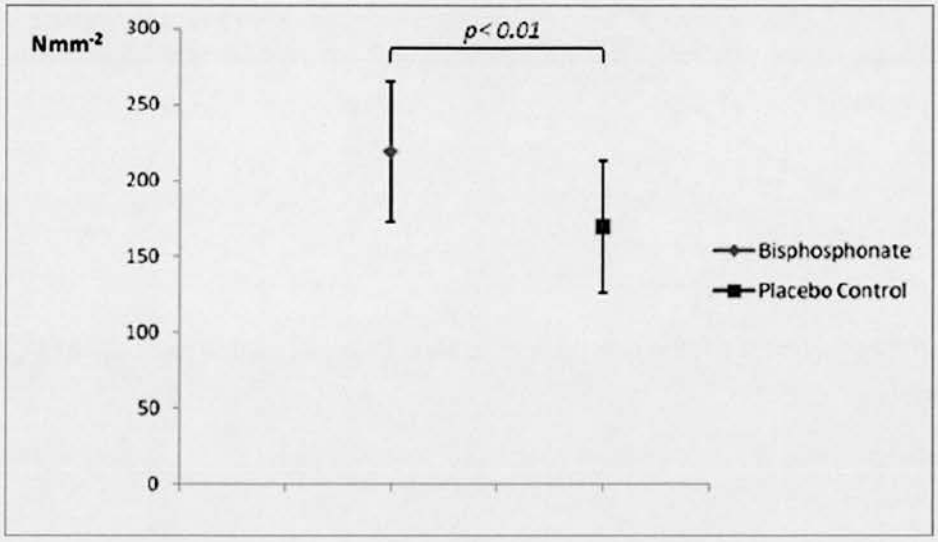

Chart 7: Mean bending stress at failure following application of a 4-point bend in uninjured contra-lateral tibial diaphysis. Bars indicate (± SD).

Radiographic Analysis of Bone Density

There was no statistically significant difference in the mean (±SD) Al.Eq density at the tibial diaphysis [Bisphosphonate v. Placebo = 1.53(±0.24) v. 1.76(±0.33)]. A scatter plot of the relationship between Al.Eq density and stress at failure is presented in Chart 8. Regression lines plotted on Microsoft Excel 2007 suggest a steeper gradient for the IBAN group in comparison to the CONTROL group.

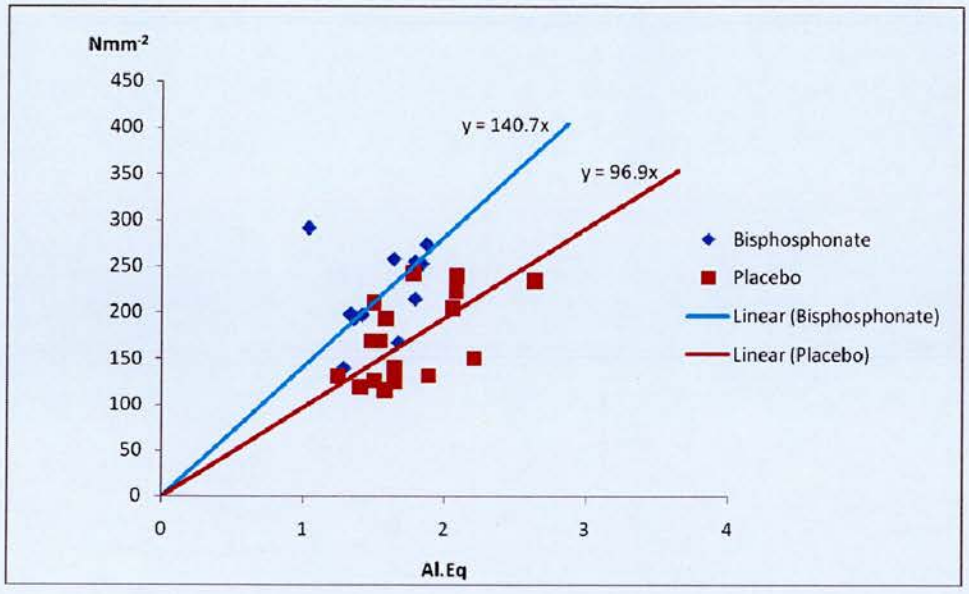

Chart 8: Scatter plot of relationship between stress at failure of cortical bone and Al.Eq density.

Discussion

A Rodent Model of Direct Fracture Healing

Previous studies of healing tibial fractures in rats have solely assessed indirect fracture healing. In this study, a model of direct fracture healing in the rat that resembles operative fracture fixation seen in routine clinical practice has been developed. A transverse tibial osteotomy is rigidly fixed with compression plating similar to that used in routine clinical practice for operative fracture management. This simple reproducible rodent model of direct fracture healing may be used in the future study of direct fracture healing.

The histological appearance of the healing rat tibial osteotomies was similar to that previously reported in the early descriptions of direct fracture healing in the dog[24,25], sheep[28] and rabbit[23,29]. 'Contact-healing' with 'cutting-cones' traversing the osteotomy predominated at the cortex adjacent to the plate and 'gap-healing' occurred at the far cortical surface with new bone formation observed to be orientated parallel to the osteotomy line.

Due to decreasing societal acceptance it is difficult to perform fracture healing studies in domestic animals. There are also fewer animal research facilities that house domestic animals. The animal costs for larger farm animals are significantly greater. The animal cost for the work carried out in this thesis would have been threefold greater if performed using rabbits. Furthermore there has been a large number of recent fracture healing studies that used rat models of indirect fracture healing[111]. The existence of a rat direct fracture healing model will permit the use of recently developed methods to study rat fracture repair to be applied to further investigations that concern direct fracture healing.

A recent plate fixation model of a mouse femoral osteotomy[92] described earlier radiological healing and greater fracture stiffness with a non-destructive bending test, in comparison to less rigid fixation with an intra-medullary device. The intra-medullary device had a cone shaped head and proximal thread to provide better rotational control of the osteotomy. Assessments were made at two and five weeks post osteotomy. On histology, some external callus was observed and no osteonal remodelling units ('cutting-cones') were demonstrated that traversed the fracture site. It may be that earlier histological analysis within the first two weeks would have revealed cartilage. A previous model of intramedullary fixation in murine tibial fractures found that the slope for the proportion of cartilage composition within the fracture callus was increased up to day-7. There was a continued increase in the proportion of cartilage with a decreased gradient in the slope up to day-9 post fracture and a reduction by the next measurement at day-14 post fracture. This indicated that the peak cartilage content would have been observed at a point between day-7 and day-14 post fracture. The reported ultimate bending load and bending stiffness in this study increased sharply from day-7 onwards which would be consistent with the commencement of callus mineralisation and decrease in cartilage deposition as found on histology[91]. A similar observed improvement in mechanical properties of murine fractures have also been reported by Cheung et al[94] in a model of external fixation after day-7 post fracture. The model of Histing et al[92], therefore appears to be a good model of intramembranous ossification but not of direct fracture healing with 'cutting-cones'. They also noted surgical failure in four of 20 animals described as implant dislocation during fixation.

The model reported in this thesis reliably produced healing without callus. The observation of minimal external callus on the posterior cortex of the tibia in one animal, early in the series, may have been due to inadequate periosteal stripping adjacent to the osteotomy on the posterior tibial surface. This area was difficult to visualise fully. However, adequate stripping of the periosteum here may be especially important due to the broad attachment of the deep posterior compartment muscles to the posterior tibia. Therefore, care should be taken to ensure the periosteum is stripped adjacent to the osteotomy, in particular on the posterior tibial cortex. In this study the length of periosteum for only one diameter of the bone width at the osteotomy was stripped on either side of the osteotomy. This was to prevent excessive disruption to the periosteal blood supply and is less than the periosteal stripping of twice the diameter of bone that was performed by Rahn et al[23] and Ashhurst et al[29] in the previously described model of direct fracture healing in the rabbit.

Indirect fracture healing via callus formation in the long bone of an adult rat has been reported to take up to 12 weeks prior to the restoration of mechanical properties similar to the uninjured side[148]. The process of direct fracture healing proceeds to completion through a lengthier time course[1,3]. Therefore, at six weeks post fracture fixation the strength of the rigidly fixed healing tibial osteotomies would not be expected to be similar to that of the contra-lateral limb. At the six week stage the mean load of failure of the rigidly plated rat tibial osteotomies in this study was similar to the mean value of 27.5 N as previously reported in a model of non-rigidly fixed healing rat tibial osteotomies[61]. The values for stress at failure of the healing osteotomies were similar to that obtained by Bak et al.[99] via three-point bending in

their rat tibial fracture model that healed with callus formation. At six weeks Bak et al[99] noted a mean proportional strength of 12.2% for their healing fractures compared to the contra-lateral tibia. The mean proportional strength of the rigidly plated healing rat tibial osteotomies within the plate control group, in this study was 15.2%. Therefore the rigid plating model that has been developed enables direct fracture repair that is quantifiable in 4-point bending tests with failure load values at six weeks post plating that are comparable to that which has been previously reported in non-rigid fracture repair models in the rat.

The surgical procedure could be simplified by the development of a miniature dynamic compression plate that is comprised of oval holes with sloped edges. The finding that direct fracture healing occurs in the rat as seen in this study may be justification for future work to refine the plate as this may enable fixation of rodent tibial fractures of differing configurations with greater ease.

The Effects of Bisphosphonates on Direct Fracture Healing

There have been no papers describing the effects of bisphosphonate on fracture healing with plate fixation. There is however one published abstract on this topic[110]. Cynomolgous monkeys were administered alendronate, a nitrogen containing bisphosphonate, in a low and high dose for three weeks prior to femoral osteotomy and plating. Alendronate therapy was continued post femoral plating for a further 26 weeks. The authors report that stress at failure following a high dose of alendronate therapy was significantly lower than controls. In both alendronate treatment groups there was a larger callus volume, with a greater proportion of woven to lamellar bone and decreased bone formation rate. The abstract does not provide any detail on the plate used for fracture stabilisation and does not mention rigid fixation. It is of particular note that the abstract suggests that all animals had visible external callus formation indicating that this was therefore not a model of direct fracture healing.

Here a model of rigid tibial plating has been used where no external callus was noted on serial radiographs of all animals in the control group and bone repair occurred by direct healing with 'cutting-cones' tunnelling across the fracture site. In addition the effects of bisphosphonate therapy has been assessed in a model of non-rigid fixation, where an external fixator was used to stabilise a standardised tibial osteotomy using a similar surgical approach and the same number and size of screw holes for bone fixation.

In the direct fracture healing group, animals treated with bisphosphonate had a statistically significant lower mean stress at failure of the healing osteotomies.

Furthermore, in the bisphosphonate treated animals the fracture line was more clearly visible and the histological appearance of predominantly cartilage and undifferentiated mesenchymal tissue with a lack of new bone formation was indicative of impaired fracture healing.

These findings suggest that bisphosphonate treatment in a therapeutic dose, as used for fragility fracture risk reduction in osteoporosis, had an inhibitory effect on direct fracture healing as evident on mechanical testing, radiographs and histology.

The Effects of Bisphosphonate on Indirect Fracture Healing

There was no significant difference in the radiological and histological appearance of the non-rigidly fixed healing osteotomies between the bisphosphonate treated animals and controls. Due to post-operative complications there were insufficient animal numbers for meaningful comparison of the bisphosphonate effect on the mechanical properties of the healing osteotomies in the indirect fracture healing group but reports in the literature[19,59,67,68] indicate that bisphosphonate administration in a therapeutic dose does not impair the mechanical properties of healing fractures and results in a larger external callus bulk.

It has been suggested that callus size peaks at a point that coincides with callus remodelling. This is based on serial measurements of increasing callus size on radiographs in association with improved patient function[5,128], increased in vivo fracture stability in a clinical study[5] and on increasing failure load of experimental tibial fractures[129]. The timing of the peak in callus size at day-21 post experimental tibial fractures that corresponds with the initial peak fracture failure load has been observed to coincide with the onset of callus remodelling on histological assessment of healing experimental tibial fractures[2].

The finding that callus index peaks at between four to six weeks post-fracture in the non-rigidly fixed controls but continued to rise up to six weeks post-fracture in the bisphosphonate treated animals suggests that bisphosphonate treatment delays the onset of callus remodelling. This is in keeping with previously published findings that indicate bisphosphonate treatment delays callus remodelling[19,20,67,68,71] in indirect

fracture healing where there is a larger callus size and the persistence of a greater proportion of woven to lamellar bone later during the fracture repair process.

Clinical Relevance of Bisphosphonate Inhibitory Effect on Direct Fracture Healing

Currently displaced forearm diaphyseal fractures in adults are nearly always treated with anatomical reduction and rigid fixation whereby direct fracture healing predominates. This is to permit early mobilisation of the upper extremity and enhance functional recovery. The presence of external callus may cause a mechanical block to forearm rotation with corresponding functional restrictions. Displaced humeral shaft fractures may be treated with rigid plate fixation. Recent clinical studies suggest that humeral plating is associated with less perioperative complications in comparison to non-rigid, intramedullary nail fixation but with similar longer term functional scores[149,150]. The AO philosophy that largely influences operative fracture treatment recommends anatomical reduction and rigid fixation of articular fractures to prevent premature articular cartilage degeneration as a result of abnormal point loading with a malunited fracture[31].

Over a one year period at the Trauma Unit of the Edinburgh Royal Infirmary between 4th July 2007 and 3rd July 2008 there were 67 adult forearm diaphyseal fractures and 66 humeral diaphyseal fractures treated. The following two graphs show the distribution of humeral and forearm diaphyseal fractures in relation to age and gender.

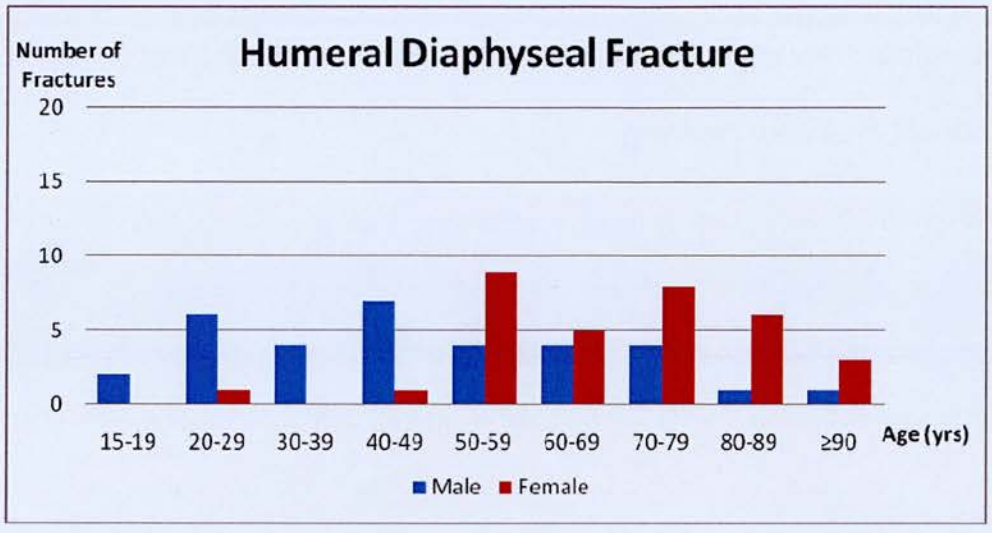

Chart 9: Age and gender distribution of humeral diaphyseal fractures treated at the Edinburgh Royal Infirmary between 4th July 2007 and 3rd July 2008

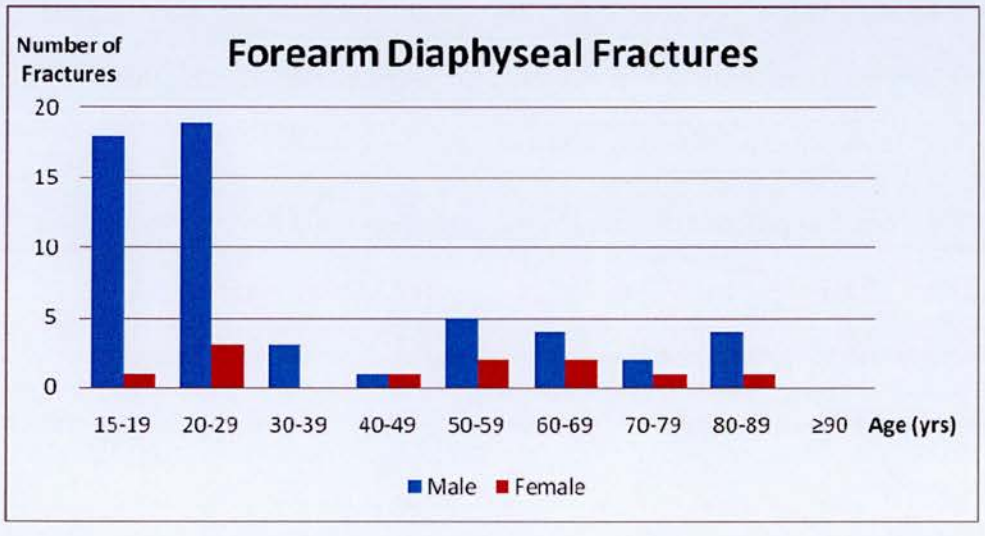

Chart 10: Age and gender distribution of forearm diaphyseal fractures treated at the Edinburgh Royal Infirmary between 4th July 2007 and 3rd July 2008

From the above graphs it is noticeable that for both these fracture types the frequency for females was greater in the above 50 years age group that suggests

these fractures may be related to post-menopausal osteoporosis. 45(68.2%) of 66 humeral diaphyseal fractures occurred in patients 50 years of age or older, and of these, greater than two-thirds (31) of fractures were in women. A proportion of these fractures would have been treated surgically and may have occurred in patients on bisphosphonate treatment where information on the effects of bisphosphonates on direct fracture healing may have influenced the trauma surgeon's treatment.

Prospectively collected data from 1364 consecutive patients over the age of 55 years that presented from the community to the Trauma Unit at The Edinburgh Royal Infirmary with hip fractures between 5th June 2007 to 26th March 2009, revealed that 71 patients (5.2%) were on bisphosphonate treatment prior to their fracture. In line with current recommendations for secondary prevention of fragility fractures[48,49] bisphosphonate uptake is likely to increase. Plated humeral and forearm diaphyseal fractures of radius and ulna, in patients receiving bisphosphonates may be at particular risk of non-union. In these patients if a rigid mode of fracture healing is optimal it may be essential to overcome the local osteoclastic inhibition for instance by adding bone graft or growth factors

In instances where operative fracture stabilisation is required for fractures in patients that are already on bisphosphonate treatment, orthopaedic surgeons may need to consider using non-rigid modes of fixation when possible. The surgeon may also consider temporarily discontinuing bisphosphonate therapy during the initial period of direct fracture healing. More importantly, however it is proposed that bisphosphonate therapy not be commenced immediately after a fracture that is rigidly fixed.

The Effect of Bisphosphonate on the Uninjured Contra-lateral Limb

There is conflicting evidence regarding the effect of bisphosphonates on the mechanical properties of cortical bone. In growing rats, both a short bisphosphonate treatment period of three weeks with pamidronate [151], and a longer duration of up to two years with alendronate [85] have been shown to increase femoral cortical strength in three-point bending stress tests compared to healthy controls. In ovariectomised rats, three months of clodronate[152] and one year of zolendronic acid[121] increased femoral[121,152] and tibial[152] cortical bending strength in comparison to sham-ovariectomised controls. However, six months of alendronate therapy in ovariectomised rats did not affect femoral diaphyseal strength in bending tests despite the increased mechanical strength noted in cancellous bone tested in compression[84]. Similarly, six months of alendronate[120] in castrated male rats did not increase bending strength of the femur diaphysis, despite the enhanced strength noted previously in ovariectomised rats that received a similar dosing regimen[85].

The differing results may be because previous studies in rodents have used ovariectomised[84,121,152] castrated, [120] or skeletally immature[85,120,151] models. Following ovariectomy there is increased bone formation in the rat tibial diaphysis[153], and up to six months following ovariectomy tibial bending strength remains elevated compared to sham-ovariectomised rats[152]. Therefore, an ovariectomised model was not used as it may have confounded our results. The effect of orchidectomy on bone properties are only noted from four months post

castration onwards [154,155]. This factor was not incorporated in to the experimental protocol of the study by Broulik et al.[120] that used castrated animals.

There is no previously published study that has used mature ex-breeder animals which would be more representative of the situation in routine clinical practice when bisphosphonates are frequently prescribed for the prevention of fragility fractures in the elderly population. Skeletally mature animals were also used to eliminate possible differing bisphosphonate effects on growing bone.

Osteopenia is known to occur during the fracture healing process [76,90]. Our results indicate that ibandronate therapy at a dose known to preserve cancellous bone BMD and strength[143] may increase cortical bone stress at failure. This finding differs to that previously reported in a beagle dog model of long bone fracture, where alendronate therapy at a high non-therapeutic dose had no significant effect on the stress at failure either of the healing fractured radius or the contra-lateral bone[70].

This study suggests that within nine weeks of ibandronate therapy the mean stress at failure of cortical bone is increased by greater than 20%. There was also no difference in the cortical bone physical dimensions. If the regions of bone that are undergoing remodelling by osteoclasts are not contributing to the mechanical strength of the bone, then the rapid increase in bone strength with bisphosphonate treatment could be accounted for by these regions now being able to contribute to the strength of the bone, as they are no longer being resorbed by osteoclasts.

A previous study using cortical femoral specimens from human donors reported a linear relationship between the decrease in bone strength and toughness with aging[156]. The authors concluded that in respect to age related change in bone material

properties the relationship between bone strength and toughness was linear, similar to that seen in synthetic fibre composites[157]. In the current study, despite an increase in bone strength of more than 20% following nine weeks of bisphosphonate therapy, the bone toughness and work-to-failure was not significantly changed, suggesting that the energy absorbed per unit of bone prior to failure changed less than the absolute strength.

Despite the significant positive effect of ibandronate therapy on the stress at failure of rat tibial diaphyses in bending tests, no statistically significant effect was noted in the radiological assessment of bone density. This may be due to remodelling areas not contributing mechanically but still contributing to radiographic bone density. Alternatively, the mechanical properties may be altered prior to detectable radiographic change. Whatever the cause for the increase in strength, the observed bisphosphonate effect on mechanical properties of the uninjured limb needs to be considered when reporting proportional strength of fracture repair compared to the unfractured limb.

This study has demonstrated that ibandronate therapy increased the stress at failure of cortical bone in the uninjured limb in the early phase following a fracture. It is increasingly evident that a large proportion of osteoporotic fractures occur at non-vertebral sites where cortical bone is the predominant material present and is due to the significant cortical bone loss that occurs in osteoporosis [158]. The observed increase in stress at failure of cortical bone with ibandronate treatment is encouraging. However, the lack of a similar beneficial effect on bone toughness and work-to-failure should be borne in mind.

Following prolonged bisphosphonate therapy the adverse effects of bisphosphonates on bone remodelling, especially in cortical bone[78], with the resultant accumulation of 'microcracks' may make the bone prone to brittle fractures. This is becoming clinically apparent. In a recent clinical case series, Odvina et al[78] reported spontaneous non-vertebral fractures in nine patients on continuous alendronate treatment for between three to eight years. Five of these patients had femoral shaft fractures. Bone biopsies from the iliac crest showed reduced surface osteoclast and osteoblast with decreased tetracycline labelling suggesting impaired bone turnover. Radiographs revealed delayed bone healing.

The low energy, 'atypical' subtrochanteric femur fracture is emerging as an entity seen following prolonged alendronate treatment. Goh et al.[77] retrospectively reviewed 13 low energy subtrochanteric femur fractures that presented to their hospital over a 10 month period in 2007 and noted that nine of these patients were on continuous alendronate treatment for between 2 ½ to 5 years. They comment on the distinctive unicortical beaking on the lateral tension surface of the femur and prodromal thigh pain that may be noticed prior to the fracture. Neviaser et al[79] retrospectively reviewed all 70 low energy femoral shaft fractures that presented to their unit over a five year period. They found that 25(36%) of these fractures occurred in patients on alendronate therapy. 19(75%) of these 25 patients exhibited a unicortical beak on radiographs with surrounding cortical hypertrophy.

The effects of longer term bisphosphonate therapy needs further study. Bisphosphonates have been proven to have a role in fragility fracture prevention, however an improved understanding of dosing regimens is needed to prevent, potentially avoidable fractures in patients on bisphosphonate therapy.

Conclusions

A simple reproducible rodent model of direct fracture healing has been developed. This model may be used for future studies concerning direct fracture healing.

The results of this study have shown that within 9 weeks of ibandronate therapy the stress at failure of rodent cortical bone was significantly increased compared to controls that received a placebo. This bisphosphonate related increase in the strength of the contra-lateral limb should be considered when reporting the strength of fracture repair. Commonly the mechanical testing results of fracture repair are reported as a proportion to that of the uninjured limb. Changes in the uninjured limb could therefore confound the results of fracture repair when expressed as a ratio.

In the rodent model, ibandronate therapy inhibited direct fracture healing. This was demonstrated based on mechanical testing, on the appearance of plain radiographs and on histological analysis. This has implications for the orthopaedic surgeon on the choice of surgical fixation method during the operative stabilisation of fractures in patients that are on bisphosphonate therapy.

Future Research and Further Work

The effect of timing of bisphosphonate administration relative to the direct fracture healing process is not known. Orthopaedic surgeons face the clinical scenario of patients already on bisphosphonate therapy prior to fracture that requires rigid plating. The surgeon will need to decide on whether discontinuing bisphosphonate treatment prior to surgery will eliminate its inhibitory effect on direct fracture healing or whether a non-rigid fixation modality should be used. Further investigation is required to ascertain if there is any worthwhile recovery of osteoclast function in animals already on bisphosphonates when they fracture provided the bisphosphonate is stopped at the time of fracture. In situations where rigid fixation is essential in patients on bisphosphonate treatment local or systemic adjuncts to reduce its negative effect on direct fracture healing will require study.

Further study is required to assess commencement of bisphosphonate therapy post rigid fracture fixation to investigate the clinical scenario where a patient who is not on bisphosphonates sustains a fragility fracture and the treating surgeon needs to decide whether early commencement of bisphosphonate as secondary fracture prevention may be detrimental to the healing process of the current fracture.

References

1. McKibbin B. The biology of fracture healing in long bones. *J Bone Joint Surg Br 1978;60-B-2:150-62.*

2. Schindeler A, McDonald MM, Bokko P, Little DG. Bone remodeling during fracture repair: The cellular picture. *Semin Cell Dev Biol 2008;19-5:459-66.*

3. Shapiro F. Bone development and its relation to fracture repair. The role of mesenchymal osteoblasts and surface osteoblasts. *Eur Cell Mater 2008;15:53-76.*

4. Goodship AE, Kenwright J. The influence of induced micromovement upon the healing of experimental tibial fractures. *J Bone Joint Surg Br 1985;67-4:650-5.*

5. Gardner TN, Hardy J, Evans M, Kenwright J. Temporal changes in dynamic inter fragmentary motion and callus formation in fractures. *J Biomech 1997;30-4:315-21.*

6. Ham AW, Harris WR. Repair and Transplantation of Bone. In: Bourne GH, ed. *The Biochemistry and Physiology of Bone.* New York: Academic Press Inc, 1956.

7. Barnes GL, Kostenuik PJ, Gerstenfeld LC, Einhorn TA. Growth factor regulation of fracture repair. *J Bone Miner Res 1999;14-11:1805-15.*

8. McDonald MM, Morse A, Mikulec K, Godfrey C, Sztynda T, Little DG. The osteopetrotic Incisor absent rat exhibits reduced osteoclast activity, resulting in normal endochondral fracture union but delayed hard callus remodelling. *J Bone Miner Res 2007;22-Suppl 1:S253.*

9. Flick LM, Weaver JM, Ulrich-Vinther M, Abuzzahab F, Zhang X, Dougall WC, Anderson D, O'Keefe RJ, Schwarz EM. Effects of receptor activator of NFkappaB (RANK) signaling blockade on fracture healing. *J Orthop Res 2003;21-4:676-84.*

10. Behonick DJ, Xing Z, Lieu S, Buckley JM, Lotz JC, Marcucio RS, Werb Z, Miclau T, Colnot C. Role of matrix metalloproteinase 13 in both endochondral and intramembranous ossification during skeletal regeneration. *PLoS One 2007;2-11:e1150.*

11. Colnot C, Thompson Z, Miclau T, Werb Z, Helms JA. Altered fracture repair in the absence of MMP9. *Development 2003;130-17:4123-33.*

12. Thompson Z, Miclau T, Hu D, Helms JA. A model for intramembranous ossification during fracture healing. *J Orthop Res 2002;20-5:1091-8.*

13. Bourque WT, Gross M, Hall BK. A reproducible method for producing and quantifying the stages of fracture repair. *Lab Anim Sci 1992;42-4:369-74.*

14. Tang Y, Nakada MT, Kesavan P, McCabe F, Millar H, Rafferty P, Bugelski P, Yan L. Extracellular matrix metalloproteinase inducer stimulates tumor angiogenesis by elevating vascular endothelial cell growth factor and matrix metalloproteinases. *Cancer Res 2005;65-8:3193-9.*

15. Nakase T, Yoshikawa H. Potential roles of bone morphogenetic proteins (BMPs) in skeletal repair and regeneration. *J Bone Miner Metab 2006;24-6:425-33.*

16. Tanaka S, Takahashi N, Udagawa N, Tamura T, Akatsu T, Stanley ER, Kurokawa T, Suda T. Macrophage colony-stimulating factor is indispensable for

both proliferation and differentiation of osteoclast progenitors. *J Clin Invest 1993;91-1:257-63.*

17. Kong YY, Yoshida H, Sarosi I, Tan HL, Timms E, Capparelli C, Morony S, Oliveira-dos-Santos AJ, Van G, Itie A, Khoo W, Wakeham A, Dunstan CR, Lacey DL, Mak TW, Boyle WJ, Penninger JM. OPGL is a key regulator of osteoclastogenesis, lymphocyte development and lymph-node organogenesis. *Nature 1999;397-6717:315-23.*

18. Schell H, Lienau J, Epari DR, Seebeck P, Exner C, Muchow S, Bragulla H, Haas NP, Duda GN. Osteoclastic activity begins early and increases over the course of bone healing. *Bone 2006;38-4:547-54.*

19. Li J, Mori S, Kaji Y, Mashiba T, Kawanishi J, Norimatsu H. Effect of bisphosphonate (incadronate) on fracture healing of long bones in rats. *J Bone Miner Res 1999;14-6:969-79.*

20. McDonald MM, Dulai S, Godfrey C, Amanat N, Sztynda T, Little DG. Bolus or weekly zoledronic acid administration does not delay endochondral fracture repair but weekly dosing enhances delays in hard callus remodeling. *Bone 2008;43-4:653-62.*

21. Sahni M, Guenther HL, Fleisch H, Collin P, Martin TJ. Bisphosphonates act on rat bone resorption through the mediation of osteoblasts. *J Clin Invest 1993;91-5:2004-11.*

22. Perren SM. Evolution of the internal fixation of long bone fractures. The scientific basis of biological internal fixation: choosing a new balance between stability and biology. *J Bone Joint Surg Br 2002;84-8:1093-110.*

23. Rahn BA, Gallinaro P, Baltensperger A, Perren SM. Primary bone healing. An experimental study in the rabbit. *J Bone Joint Surg Am 1971;53-4:783-6.*

24. Schenk R, Willenegger H. [on the Histology of Primary Bone Healing]. *Langenbecks Arch Klin Chir Ver Dtsch Z Chir 1964;308:440-52.*

25. Olerud S, Danckwardt-Lilliestrom G. Fracture healing in compression osteosynthesis in the dog. *J Bone Joint Surg Br 1968;50-4:844-51.*

26. Perren SM. Physical and biological aspects of fracture healing with special reference to internal fixation. *Clin Orthop Relat Res 1979-138:175-96.*

27. Klaue K. Principles of plate and screw osteosynthesis. In: Bulstrode C, Buckwalter J, Carr A, Marsh L, Wilson-MacDonald J, Bowden G, eds. *Oxford textbook of orthopaedics and trauma.* Vol. 3, 1st ed. Oxford: Oxford University Press, 2002:1697-710.

28. Perren SM, Huggler A, Russenberger M, Allgower M, Mathys R, Schenk R, Willenegger H, Muller ME. The reaction of cortical bone to compression. *Acta Orthop Scand Suppl 1969;125:19-29.*

29. Ashhurst DE, Hogg J, Perren SM. A method for making reproducible experimental fractures of the rabbit tibia. *Injury 1982;14-3:236-42.*

30. Shapiro F. Cortical bone repair. The relationship of the lacunar-canalicular system and intercellular gap junctions to the repair process. *J Bone Joint Surg Am 1988;70-7:1067-81.*

31. Marsh JL, Buckwalter J, Gelberman R, Dirschl D, Olson S, Brown T, Llinias A. Articular fractures: does an anatomic reduction really change the result? *J Bone Joint Surg Am 2002;84-A-7:1259-71.*

32. Amanat N, McDonald M, Godfrey C, Bilston L, Little D. Optimal timing of a single dose of zoledronic acid to increase strength in rat fracture repair. *J Bone Miner Res 2007;22-6:867-76.*

33. Felix R, Cecchini MG, Fleisch H. Macrophage colony stimulating factor restores in vivo bone resorption in the *op/op* osteopetrotic nouse. *J Bone Miner Res 1990;5:781-88.*

34. Kanis JA. Maintenance of Bone Mass. In: *Textbook of Osteoporosis*, 1st ed. London: Blackwell Science, 1996:1-28.

35. Genuth SM. Endocrine Regulation of Calcium and Phosphate Metabolism. In: Berne RM, Levy MN, Koeppen BM, Stanton BA, eds. *Physiology*, 5th ed. St. Louis: Mosby, 2004.

36. Rogers MJ, Gordon S, Benford HL, Coxon FP, Luckman SP, Monkkonen J, Frith JC. Cellular and molecular mechanisms of action of bisphosphonates. *Cancer 2000;88-12 Suppl:2961-78.*

37. Bonucci E. New knowledge on the origin, function and fate of osteoclasts. *Clin Orthop Relat Res 1981-158:252-69.*

38. Epstein S, Zaidi M. Biological properties and mechanism of action of ibandronate: application to the treatment of osteoporosis. *Bone 2005;37-4:433-40.*

39. Ito M, Amizuka N, Nakajima T, Ozawa H. Ultrastructural and cytochemical studies on cell death of osteoclasts induced by bisphosphonate treatment. *Bone 1999;25-4:447-52.*

40. Gong L, Altman RB, Klein TE. Bisphosphonates pathway. *Pharmacogenet Genomics;21-1:50-3.*

41. Luckman SP, Coxon FP, Ebetino FH, Russell RG, Rogers MJ. Heterocycle-containing bisphosphonates cause apoptosis and inhibit bone resorption by preventing protein prenylation: evidence from structure-activity relationships in J774 macrophages. *J Bone Miner Res 1998;13-11:1668-78.*

42. Luckman SP, Hughes DE, Coxon FP, Graham R, Russell G, Rogers MJ. Nitrogen-containing bisphosphonates inhibit the mevalonate pathway and prevent post-translational prenylation of GTP-binding proteins, including Ras. *J Bone Miner Res 1998;13-4:581-9.*

43. Yue J, Zhang X, Dong B, Yang M. Statins and bone health in postmenopausal women: a systematic review of randomized controlled trials. *Menopause;17-5:1071-9.*

44. Khan SA, Kanis JA, Vasikaran S, Kline WF, Matuszewski BK, McCloskey EV, Beneton MN, Gertz BJ, Sciberras DG, Holland SD, Orgee J, Coombes GM,

Rogers SR, Porras AG. Elimination and biochemical responses to intravenous alendronate in postmenopausal osteoporosis. *J Bone Miner Res 1997;12-10:1700-7.*

45. Vitte C, Fleisch H, Guenther HL. Bisphosphonates induce osteoblasts to secrete an inhibitor of osteoclast-mediated resorption. *Endocrinology 1996;137-6:2324-33.*

46. von Knoch F, Jaquiery C, Kowalsky M, Schaeren S, Alabre C, Martin I, Rubash HE, Shanbhag AS. Effects of bisphosphonates on proliferation and osteoblast differentiation of human bone marrow stromal cells. *Biomaterials 2005;26-34:6941-9.*

47. Fleisch H. Bisphosphonates: mechanisms of action. *Endocr Rev 1998;19-1:80-100.*

48. SIGN. Guideline No. 71: Management of Osteoporosis. *Scottish Intercollegiate Guidelines Network June 2003.*

49. NICE. TA161: Alendronate, etidronate,risedronate, raloxifene, strontium ranelate and teriparatide for the secondary prevention of osteoporotic fragility fractures in postmenopausal women (amended). *National Institute for Health and Clinical Excellence Jan 2010.*

50. Adami S. Bisphosphonate antifracture efficacy. *Bone 2007;41-5, Supplement 1:S8-S15.*

51. Wasnich RD, Miller PD. Antifracture efficacy of antiresorptive agents are related to changes in bone density. *J Clin Endocrinol Metab 2000;85-1:231-6.*

52. Black DM, Cummings SR, Karpf DB, Cauley JA, Thompson DE, Nevitt MC, Bauer DC, Genant HK, Haskell WL, Marcus R, Ott SM, Torner JC, Quandt SA, Reiss TF, Ensrud KE. Randomised trial of effect of alendronate on risk of fracture in women with existing vertebral fractures. Fracture Intervention Trial Research Group. *Lancet 1996;348-9041:1535-41.*

53. Bone HG, Hosking D, Devogelaer JP, Tucci JR, Emkey RD, Tonino RP, Rodriguez-Portales JA, Downs RW, Gupta J, Santora AC, Liberman UA. Ten years' experience with alendronate for osteoporosis in postmenopausal women. *N Engl J Med 2004;350-12:1189-99.*

54. Chesnut IC, Skag A, Christiansen C, Recker R, Stakkestad JA, Hoiseth A, Felsenberg D, Huss H, Gilbride J, Schimmer RC, Delmas PD. Effects of oral ibandronate administered daily or intermittently on fracture risk in postmenopausal osteoporosis. *J Bone Miner Res 2004;19-8:1241-9.*

55. Orwoll ES, Binkley NC, Lewiecki EM, Gruntmanis U, Fries MA, Dasic G. Efficacy and safety of monthly ibandronate in men with low bone density. *Bone;46-4:970-6.*

56. Lewiecki EM, Keaveny TM, Kopperdahl DL, Genant HK, Engelke K, Fuerst T, Kivitz A, Davies RY, Fitzpatrick LA. Once-monthly oral ibandronate improves biomechanical determinants of bone strength in women with postmenopausal osteoporosis. *J Clin Endocrinol Metab 2009;94-1:171-80.*

57. McLung MR, Wasnich RD, Recker R, Cauley JA, Chesnut IC, Ensrud KE, Burdeska A, Mills T. Oral Daily Ibandronate Prevents Bone Loss in Early Postmenopausal Women Without Osteoporosis. *J Bone Miner Res 2004;19:11-8.*

58. Amanat N, Brown R, Bilston LE, Little DG. A single systemic dose of pamidronate improves bone mineral content and accelerates restoration of strength in a rat model of fracture repair. *J Orthop Res 2005;23-5:1029-34.*

59. Cao Y, Mori S, Mashiba T, Westmore MS, Ma L, Sato M, Akiyama T, Shi L, Komatsubara S, Miyamoto K, Norimatsu H. Raloxifene, estrogen, and alendronate affect the processes of fracture repair differently in ovariectomized rats. *J Bone Miner Res 2002;17-12:2237-46.*

60. Hyvonen PM, Karhi T, Kosma VM, Liimola-Luoma L, Hanhijarvi H. The influence of dichloromethylene bisphosphonate on the healing of a long bone fracture, composition of bone mineral and histology of bone in the rat. *Pharmacol Toxicol 1994;75-6:384-90.*

61. Koivukangas A, Tuukkanen J, Kippo K, Jamsa T, Hannuniemi R, Pasanen I, Vaananen K, Jalovaara P. Long-term administration of clodronate does not prevent fracture healing in rats. *Clin Orthop Relat Res 2003-408:268-78.*

62. Li C, Mori S, Li J, Kaji Y, Akiyama T, Kawanishi J, Norimatsu H. Long-term effect of incadronate disodium (YM-175) on fracture healing of femoral shaft in growing rats. *J Bone Miner Res 2001;16-3:429-36.*

63. Li J, Mori S, Kaji Y, Kawanishi J, Akiyama T, Norimatsu H. Concentration of bisphosphonate (incadronate) in callus area and its effects on fracture healing in rats. *J Bone Miner Res 2000;15-10:2042-51.*

64. Madsen JE, Berg-Larsen T, Kirkeby OJ, Falch JA, Nordsletten L. No adverse effects of clodronate on fracture healing in rats. *Acta Orthop Scand 1998;69-5:532-6.*

65. Nyman MT, Gao T, Lindholm TC, Lindholm TS. Healing of a tibial double osteotomy is modified by clodronate administration. *Arch Orthop Trauma Surg 1996;115-2:111-4.*

66. Nyman MT, Paavolainen P, Lindholm TS. Clodronate increases the calcium content in fracture callus. An experimental study in rats. *Arch Orthop Trauma Surg 1993;112-5:228-31.*

67. Tarvainen R, Olkkonen H, Nevalainen T, Hyvonen P, Arnala I, Alhava E. Effect of clodronate on fracture healing in denervated rats. *Bone 1994;15-6:701-5.*

68. Goodship AE, Walker PC, McNally D, Chambers T, Green JR. Use of a bisphosphonate (pamidronate) to modulate fracture repair in ovine bone. *Ann Oncol 1994;5 Suppl 7:S53-5.*

69. Lenehan TM, Balligand M, Nunamaker DM, Wood FE, Jr. Effect of EHDP on fracture healing in dogs. *J Orthop Res 1985;3-4:499-507.*

70. Peter CP, Cook WO, Nunamaker DM, Provost MT, Seedor JG, Rodan GA. Effect of alendronate on fracture healing and bone remodeling in dogs. *J Orthop Res 1996;14-1:74-9.*

71. Li J, Mashiba T, Burr DB. Bisphosphonate treatment suppresses not only stochastic remodeling but also the targeted repair of microdamage. *Calcif Tissue Int 2001;69-5:281-6.*

72. Bauss F, Schenk RK, Hort S, Muller-Beckmann B, Sponer G. New model for simulation of fracture repair in full-grown beagle dogs: model characterization and results from a long-term study with ibandronate. *J Pharmacol Toxicol Methods 2004;50-1:25-34.*

73. Bab I, Gazit D, Massarawa A, Sela J. Removal of tibial marrow induces increased formation of bone and cartilage in rat mandibular condyle. *Calcif Tissue Int 1985;37-5:551-5.*

74. Choi JY, Kim HJ, Lee YC, Cho BO, Seong HS, Cho M, Kim SG. Inhibition of bone healing by pamidronate in calvarial bony defects. *Oral Surg Oral Med Oral Pathol Oral Radiol Endod 2007;103-3:321-8.*

75. Adolphson P, Abbaszadegan H, Boden H, Salemyr M, Henriques T. Clodronate increases mineralization of callus after Colles' fracture: a randomized, double-blind, placebo-controlled, prospective trial in 32 patients. *Acta Orthop Scand 2000;71-2:195-200.*

76. van der Poest Clement E, Patka P, Vandormael K, Haarman H, Lips P. The effect of alendronate on bone mass after distal forearm fracture. *J Bone Miner Res 2000;15-3:586-93.*

77. Goh SK, Yang KY, Koh JS, Wong MK, Chua SY, Chua DT, Howe TS. Subtrochanteric insufficiency fractures in patients on alendronate therapy: a caution. *J Bone Joint Surg Br 2007;89-3:349-53.*

78. Odvina CV, Zerwekh JE, Rao DS, Maalouf N, Gottschalk FA, Pak CY. Severely suppressed bone turnover: a potential complication of alendronate therapy. *J Clin Endocrinol Metab 2005;90-3:1294-301.*

79. Neviaser AS, Lane JM, Lenart BA, Edobor-Osula F, Lorich DG. Low-energy femoral shaft fractures associated with alendronate use. *J Orthop Trauma 2008;22-5:346-50.*

80. Bauer DC, Black DM, Garnero P, Hochberg M, Ott S, Orloff J, Thomson DE, Ewing SK, Delmas PD. Change in Bone Turnover and hip, non-spine and vertebral fracture in alendronate-treated women: The Fracture Intervention Trial. *J Bone Miner Res 2004;19:1250-8.*

81. Mashiba T, Hirano T, Turner CH, Forwood MR, Johnston CC, Burr DB. Suppressed bone turnover by bisphosphonates increases microdamage accumulation and reduces some biomechanical properties in dog rib. *J Bone Miner Res 2000;15-4:613-20.*

82. Allen MR, Burr DB. Three years of alendronate treatment results in similar levels of vertebral microdamage as after one year of treatment. *J Bone Miner Res 2007;22-11:1759-65.*

83. Smith SY, Recker RR, Hannan M, Muller R, Bauss F. Intermittent intravenous administration of the bisphosphonate ibandronate prevents bone loss and

maintains bone strength and quality in ovariectomized cynomolgus monkeys. *Bone 2003;32-1:45-55.*

84. Toolan BC, Shea M, Myers ER, Borchers RE, Seedor JG, Quartuccio H, Rodan G, Hayes WC. Effects of 4-amino-1-hydroxybutylidene bisphosphonate on bone biomechanics in rats. *J Bone Miner Res 1992;7-12:1399-406.*

85. Guy JA, Shea M, Peter CP, Morrissey R, Hayes WC. Continuous alendronate treatment throughout growth, maturation, and aging in the rat results in increases in bone mass and mechanical properties. *Calcif Tissue Int 1993;53-4:283-8.*

86. Lalla S, Hothorn LA, Haag N, Bader R, Bauss F. Lifelong administration of high doses of ibandronate increases bone mass and maintains bone quality of lumbar vertebrae in rats. *Osteoporos Int 1998;8-2:97-103.*

87. Muller R, Hannan M, Smith SY, Bauss F. Intermittent ibandronate preserves bone quality and bone strength in the lumbar spine after 16 months of treatment in the ovariectomized cynomolgus monkey. *J Bone Miner Res 2004;19-11:1787-96.*

88. Yoshida Y, Moriya A, Kitamura K, Inazu M, Okimoto N, Okazaki Y, Nakamura T. Responses of trabecular and cortical bone turnover and bone mass and strength to bisphosphonate YH529 in ovariohysterectomized beagles with calcium restriction. *J Bone Miner Res 1998;13-6:1011-22.*

89. Bauss F, Lalla S, Endele R, Hothorn LA. Effects of treatment with ibandronate on bone mass, architecture, biomechanical properties, and bone concentration of ibandronate in ovariectomized aged rats. *J Rheumatol 2002;29-10:2200-8.*

90. Karlsson M, Nilsson JA, Sernbo I, Redlund-Johnell I, Johnell O, Obrant KJ. Changes of bone mineral mass and soft tissue composition after hip fracture. *Bone 1996;18-1:19-22.*

91. Hiltunen A, Vuorio E, Aro HT. A standardized experimental fracture in the mouse tibia. *J Orthop Res 1993;11-2:305-12.*

92. Histing T, Garcia P, Matthys R, Leidinger M, Holstein JH, Kristen A, Pohlemann T, Menger MD. An internal locking plate to study intramembranous bone healing in a mouse femur fracture model. *J Orthop Res;28-3:397-402.*

93. Connolly CK, Li G, Bunn JR, Mushipe M, Dickson GR, Marsh DR. A reliable externally fixated murine femoral fracture model that accounts for variation in movement between animals. *J Orthop Res 2003;21-5:843-9.*

94. Cheung KM, Kaluarachi K, Andrew G, Lu W, Chan D, Cheah KS. An externally fixed femoral fracture model for mice. *J Orthop Res 2003;21-4:685-90.*

95. Campbell TM, Wong WT, Mackie EJ. Establishment of a model of cortical bone repair in mice. *Calcif Tissue Int 2003;73-1:49-55.*

96. Russell G, Tucci M, Conflitti J, Graves M, Wingerter S, Woodall J, Jr., Ragab A, Benghuzzi H. Characterization of a femoral segmental nonunion model in laboratory rats: report of a novel surgical technique. *J Invest Surg 2007;20-4:249-55.*

97. Bonnarens F, Einhorn TA. Production of a standard closed fracture in laboratory animal bone. *J Orthop Res 1984;2-1:97-101.*

98. An Y, Friedman RJ, Parent T, Draughn RA. Production of a standard closed fracture in the rat tibia. *J Orthop Trauma 1994;8-2:111-5.*

99. Bak B, Andreassen TT. The effect of aging on fracture healing in the rat. *Calcif Tissue Int 1989;45-5:292-7.*

100. Schmidmaier G, Wildemann B, Melis B, Krummrey G, Einhorn TA, Haas NP, Raschke M. Development and Characterization of a Standardized Closed Tibial Fracture Model in The Rat. *European Journal of Trauma 2004;30-1:35-42.*

101. Utvag SE, Grundnes O, Reikeras O. Healing of segmental and simple fractures in rats. *Acta Orthop Scand 1994;65-5:559-63.*

102. Thaller SR, Hoyt J, Tesluk H, Stevenson TR. Midfacial fracture repair in the adult rat. *Ann Plast Surg 1993;31-1:66-71.*

103. Mark H, Bergholm J, Nilsson A, Rydevik B, Stromberg L. An external fixation method and device to study fracture healing in rats. *Acta Orthop Scand 2003;74-4:476-82.*

104. Brighton CT, Hozack WJ, Brager MD, Windsor RE, Pollack SR, Vreslovic EJ, Kotwick JE. Fracture healing in the rabbit fibula when subjected to various capacitively coupled electrical fields. *J Orthop Res 1985;3-3:331-40.*

105. Henry WB, Jr., Schachar NS, Wadsworth PL, Castronovo FP, Jr., Mankin HJ. Feline model for the study of frozen osteoarticular hemijoint transplantation: qualitative and quantitative assessment of bone healing. *Am J Vet Res 1985;46-8:1714-20.*

106. Schenk RK, Willenegger HR. [Histology of primary bone healing: modifications and limits of recovery of gaps in relation to extent of the defect (author's transl)]. *Unfallheilkunde 1977;80-5:155-60.*

107. Cheal EJ, Mansmann KA, DiGioia AM, 3rd, Hayes WC, Perren SM. Role of interfragmentary strain in fracture healing: ovine model of a healing osteotomy. *J Orthop Res 1991;9-1:131-42.*

108. Nunamaker DM, Richardson DW, Butterweck DM. Mechanical and biological effects of plate luting. *J Orthop Trauma 1991;5-2:138-45.*

109. Ominsky MS, Li C, Li X, Tan HL, Lee E, Barrero M, Asuncion FJ, Dwyer D, Han CY, Vlasseros F, Samadfam R, Jolette J, Smith SY, Stolina M, Lacey DL, Simonet WS, Paszty C, Li G, Ke HZ. Inhibition of sclerostin by monoclonal antibody enhances bone healing and improves bone density and strength of non-fractured bones. *J Bone Miner Res.*

110. Cao Y, Mori S, Mashiba T, Komatsubara S, Kaji Y, Kawanishi J, Akiyama T, Miyamoto K, Iwata K, Norimatsu H. The effects of alendronate on the processes of fracture healing in weight-bearing femora of cynomolgus monkeys. *Journal of the Japanese Orthopaedic Association 2003;77-8:S1094.*

111. O'Loughlin PF, Morr S, Bogunovic L, Kim AD, Park B, Lane JM. Selection and development of preclinical models in fracture-healing research. *J Bone Joint Surg Am 2008;90 Suppl 1:79-84.*

112. Nunamaker DM. Experimental models of fracture repair. *Clin Orthop Relat Res 1998-355 Suppl:S56-65.*

113. Turner CH, Burr DB. Basic biomechanical measurements of bone: a tutorial. *Bone 1993;14-4:595-608.*

114. Bentolila V, Boyce TM, Fyhrie DP, Drumb R, Skerry TM, Schaffler MB. Intracortical remodeling in adult rat long bones after fatigue loading. *Bone 1998;23-3:275-81.*

115. Bak B, Jensen KS. Standardization of tibial fractures in the rat. *Bone 1992;13-4:289-95.*

116. Uhthoff HK, Dubuc FL. Bone structure changes in the dog under rigid internal fixation. *Clin Orthop Relat Res 1971;81:165-70.*

117. Horn J, Steen H, Reikeras O. Role of the fibula in lower leg fractures: An in vivo investigation in rats. *J Orthop Res 2008;26-7:1027-31.*

118. Shefelbine SJ, Augat P, Claes L, Beck A. Intact fibula improves fracture healing in a rat tibia osteotomy model. *J Orthop Res 2005;23-2:489-93.*

119. Madsen JE, Hukkanen M, Aune AK, Basran I, Moller JF, Polak JM, Nordsletten L. Fracture healing and callus innervation after peripheral nerve resection in rats. *Clin Orthop Relat Res 1998-351:230-40.*

120. Broulik PD, Rosenkrancova J, Ruzicka P, Sedlacek R. Effect of alendronate administration on bone mineral density and bone strength in castrated rats. *Horm Metab Res 2005;37-7:414-8.*

121. Hornby SB, Evans GP, Hornby SL, Pataki A, Glatt M, Green JR. Long-term zoledronic acid treatment increases bone structure and mechanical strength of long bones of ovariectomized adult rats. *Calcif Tissue Int 2003;72-4:519-27.*

122. Draper ER, Goodship AE. A novel technique for four-point bending of small bone samples with semi-automatic analysis. *J Biomech 2003;36-10:1497-502.*

123. Augat P, Claes L. Increased cortical remodeling after osteotomy causes posttraumatic osteopenia. *Bone 2008;43-3:539-43.*

124. Park HC, Lakes RS. Cosserat micromechanics of human bone: strain redistribution by a hydration sensitive constituent. *J Biomech 1986;19-5:385-97.*

125. Burstein AH, Currey JD, Frankel VH, Reilly DT. The ultimate properties of bone tissue: the effects of yielding. *J Biomech 1972;5-1:35-44.*

126. Sedlin ED, Hirsch C. Factors affecting the determination of the physical properties of femoral cortical bone. *Acta Orthop Scand 1966;37-1:29-48.*

127. Wright TM, Hayes WC. Tensile testing of bone over a wide range of strain rates: effects of strain rate, microstructure and density. *Med Biol Eng 1976;14-6:671-80.*

128. Eastaugh-Waring SJ, Joslin CC, Hardy JR, Cunningham JL. Quantification of fracture healing from radiographs using the maximum callus index. *Clin Orthop Relat Res 2009;467-8:1986-91.*

129. Lindsay MK, Howes EL. The breaking strength of healing fractures. *J Bone Joint Surg Am 1931;13:491-510.*

130. Blokhuis TJ, de Bruine JHD, Bramer JAM, den Boer FC, Bakker FC, Patka P, Haarman HJTM, Manoliu RA. The reliability of plain radiography in experimental fracture healing. *Skeletal Radiology 2001;30:151-6.*

131. Werner M, Chott A, Fabiano A, Battifora H. Effect of formalin tissue fixation and processing on immunohistochemistry. *Am J Surg Pathol 2000;24-7:1016-9.*

132. Helander KG. Kinetic studies of formaldehyde binding in tissue. *Biotech Histochem 1994;69-3:177-9.*

133. Skinner RA. Decalcification of Bone Tissue. In: An YH, Martin KL, eds. *Handbook of Histology Methods for Bone and Cartilage* 1st ed: Humana Press, 2003:588.

134. Sreebny LM, Nikiforuk G. Demineralization of hard tissues by organic chelating agents. *Science 1951;113-2941:560.*

135. Baumbach B, Sharkey N, Korzick D. The Effects of Endurance Exercise on the size and strength of adult and aged rat femora and tibiae. *Summer Bioengineering Conference, American Society of Mechanical Engineers.* Sonesta Beach Resort, Key Biscayne, Florida, 2003.

136. Disegi JA, Eschbach L. Stainless steel in bone surgery. *Injury 2000;31 Suppl 4:2-6.*

137. Krause WR, Bradbury DW, Kelly JE, Lunceford EM. Temperature elevations in orthopaedic cutting operations. *J Biomech 1982;15-4:267-75.*

138. Timoshenko S, Goodier JM. *Theory of Elasticity.* 2nd ed. New York: McGraw-Hill Book Company, Inc, 1951.

139. Nunamaker DM, Perren SM. A radiological and histological analysis of fracture healing using prebending of compression plates. *Clin Orthop Relat Res 1979-138:167-74.*

140. Reed AA, Joyner CJ, Isefuku S, Brownlow HC, Simpson AH. Vascularity in a new model of atrophic nonunion. *J Bone Joint Surg Br 2003;85-4:604-10.*

141. Gisby J, Beale AS, Bryant JE, Toseland CD. Staphylococcal osteomyelitis--a comparison of co-amoxiclav with clindamycin and flucloxacillin in an experimental rat model. *J Antimicrob Chemother 1994;34-5:755-64.*

142. Greene EC. Anatomy of The Rat. *Transactions of the American Philosophical Society 1959;27:56-83.*

143. Bauss F, Wagner M, Hothorn LH. Total administered dose of ibandronate determines its effects on bone mass and architecture in ovariectomized aged rats. *J Rheumatol 2002;29-5:990-8.*

144. Murray A. Fracture Healing in Osteopenic Bone and The Influence of Simvastatin. Vol. Doctor of Medicine Thesis. Edinburgh: The University of Edinburgh, 2005:199.

145. Roark RJ, Young WC. *Formulas for Stress and Strain.* New York: McGraw-Hill, 1975.

146. Komatsubara S, Mori S, Mashiba T, Li J, Nonaka K, Kaji Y, Akiyama T, Miyamoto K, Cao Y, Kawanishi J, Norimatsu H. Suppressed Bone Turnover by Long-Term Bisphosphonate Treatment Accumulates Microdamage but Maintains Intrinsic Material Properties in Cortical Bone of Dog Rib. *J Bone Miner Res 2004;19-6:999-1005.*

147. Dawson SP, Ross E, MacGillivray TJ, Muir AY, Simpson AHRW. The use of digital x-ray to monitor decalcification in sheep femora. *Proceedings of the World Conference in Medical Physics and Biomedical Engineering.* Munich, Germany, 2009.

148. Ekeland A, Engesoeter LB, Langeland N. Influence of age on mechanical properties of healing fractures and intact bones in rats. *Acta Orthop Scand 1982;53-4:527-34.*

149. Putti AB, Uppin RB, Putti BB. Locked intramedullary nailing versus dynamic compression plating for humeral shaft fractures. *J Orthop Surg (Hong Kong) 2009;17-2:139-41.*

150. Denies E, Nijs S, Sermon A, Broos P. Operative treatment of humeral shaft fractures. Comparison of plating and intramedullary nailing. *Acta Orthop Belg;76-6:735-42.*

151. Ferretti JL, Cointry G, Capozza R, Montuori E, Roldan E, Perez Lloret A. Biomechanical effects of the full range of useful doses of (3-amino-1-hydroxypropylidene)-1,1-bisphosphonate (APD) on femur diaphyses and cortical bone tissue in rats. *Bone Miner 1990;11-1:111-22.*

152. Kippo K, Hannuniemi R, Lauren L, Peng Z, Kuurtamo P, Virtamo T, Isaksson P, Osterman T, Vaananen HK, Sellman R. Effect of clodronate treatment on established bone loss in ovariectomized rats. *Bone 1998;23-4:333-42.*

153. Turner RT, Vandersteenhoven JJ, Bell NH. The effects of ovariectomy and 17 beta-estradiol on cortical bone histomorphometry in growing rats. *J Bone Miner Res 1987;2-2:115-22.*

154. Danielsen CC, Mosekilde L, Andreassen TT. Long-term effect of orchidectomy on cortical bone from rat femur: bone mass and mechanical properties. *Calcif Tissue Int 1992;50-2:169-74.*

155. Reim NS, Breig B, Stahr K, Eberle J, Hoeflich A, Wolf E, Erben RG. Cortical bone loss in androgen-deficient aged male rats is mainly caused by increased endocortical bone remodeling. *J Bone Miner Res 2008;23-5:694-704.*

156. Zioupos P, Currey JD. Changes in the stiffness, strength, and toughness of human cortical bone with age. *Bone 1998;22-1:57-66.*

157. Harris B, Dorey SE, Cooke RG. Strength and toughness of fibre composites. *Composites Science and Technology 1988;31:121-41.*

158. Zebaze RM, Ghasem-Zadeh A, Bohte A, Iuliano-Burns S, Mirams M, Price RI, Mackie EJ, Seeman E. Intracortical remodelling and porosity in the distal radius

and post-mortem femurs of women: a cross-sectional study. *Lancet;375-9727:1729-36.*

Appendix

Appendix 1: Specimen Automated Processing Protocol

Specimens processed in Vacuum Infiltrated Processor (VIP, Tissue Tech VIP, E300 series, Miles Inc)

Alcohol 50%, 2 hours at 35°C

Alcohol 80%, 1 hour at 35°C

Alcohol 95% 1hour at 35°C

Alcohol 100% 1hour at 35°C

Alcohol 100% 1hour at 35°C

Alcohol 100% 2 hours at 35°C

Xylene 100%, 3 changes of 1hour each

Paraffin, 4 changes of 1 hour each at 60°C

Specimens moulded in paraffin blocks

Appendix 2: Mechanical Testing Measurements

H – Histology

A – Abnormal (non-bending) Failure Mode

W – Wound Infection

Animal	Injured Limb				Uninjured Limb						
	Force at Failure (**N**)	Stress at Failure (**Nmm^{-2}**)	External, Coronal width (**mm**)	External, Sagittal width (**mm**)	Force at Failure (**N**)	Stress at Failure (**Nmm^{-2}**)	Work-to-failure (**J**)	Toughness (**$MJmm^{-3}$**)	External, Coronal width (**mm**)	External, Sagittal width (**mm**)	Density (**Al.Eq**)
C01	H	H	H	H	Not retrieved	Not retrieved	Not retrieved	Not retrieved	Not retrieved	Not retrieved	Not retrieved
C02	37.67	33.66	3.78	3.04	190.26	166.36	58.39	2.14	3.52	3.33	1.67
C03	H	H	H	H	Not retrieved	Not retrieved	Not retrieved	Not retrieved	Not retrieved	Not retrieved	Not retrieved
C04	H	H	H	H	Not retrieved	Not retrieved	Not retrieved	Not retrieved	Not retrieved	Not retrieved	Not retrieved
C05	0.09	0.08	3.49	3.18	166.51	254.45	58.39	2.27	3.83	2.55	1.79
C06	17.49	17.20	3.45	3.01	159.11	197.91	49.41	1.54	4.97	2.51	1.33
C07	19.49	12.48	4.38	3.48	207.66	252.15	55.15	1.97	4.08	2.94	1.84
C08	H	H	H	H	168.68	213.78	46.40	1.65	3.58	2.81	1.79
C09	16.53	4.98	3.33	5.61	199.75	257.21	193.20	7.23	2.81	2.94	1.64
C10	H	H	H	H	184.53	197.15	163.61	2.57	3.34	2.94	1.33
CX01	H	H	H	H	Not retrieved	Not retrieved	Not retrieved	Not retrieved	Not retrieved	Not retrieved	Not retrieved
CX02	49.16	31.50	3.67	3.57	164.61	290.83	85.19	4.07	2.76	2.70	1.03
CX03	H	H	H	H	148.24	138.77	48.16	1.36	4.64	3.01	1.28
CX04	H	H	H	H	164.68	192.39	37.58	1.30	3.67	2.95	1.35
CX05	112.31	49.58	4.79	3.75	204.27	196.53	30.45	0.80	4.77	2.72	1.41
CX06	H	H	H	H	190.35	273.10	74.66	3.25	2.41	3.03	1.87
CX07	56.29	22.28	4.52	4.10	A	A	A	A	5.05	3.16	Not assessed
CX08	12.96	11.45	4.57	4.16	A	A	A	A	4.36	3.30	Not assessed
S01	80.2	88.81	3.93	2.86	226.17	234.44	63.25	2.08	3.43	3.16	2.64
S02	H	H	H	H	193.73	209.78	47.79	1.46	5.06	2.83	1.50
S03	23.31	31.19	3.59	2.52	161.71	150.00	46.53	1.30	3.91	3.90	2.21
S04	H	H	H	H	129.11	119.27	22.60	0.71	4.37	2.89	1.40
S05	H	H	H	H	173.9	139.64	36.67	0.92	4.25	3.13	1.64
S06	45.23	22.66	4.56	3.83	139.26	131.15	77.04	2.34	3.67	3.23	1.89
S07	H	H	H	H	165.37	242.14	36.88	1.42	3.70	2.64	1.78
S08	29.57	17.06	5.04	3.27	161.71	204.51	62.86	2.06	3.87	2.59	2.06
S09	H	H	H	H	161.04	168.61	47.41	1.49	3.60	3.01	1.48
S10	25.93	27.67	2.75	3.23	184.79	193.04	53.73	1.74	3.30	3.11	1.58
SX01	H	H	H	H	123.62	115.19	31.53	0.92	3.84	3.13	1.58
SX02	18.44	23.94	4.20	3.03	169.47	130.75	38.33	0.88	4.79	2.99	1.24
SX03	H	H	H	H	175.74	238.73	66.10	2.56	2.80	2.85	2.08
SX04	H	H	H	H	148.32	124.98	43.41	1.11	4.53	3.04	1.64
SX05	W	W	2.76	3.14	Not retrieved	Not retrieved	Not retrieved	Not retrieved	Not retrieved	Not retrieved	Not retrieved
SX06	F	F	F	F	179.31	168.66	116.86	3.76	3.14	3.42	1.54
SX07	33.41	19.71	3.50	3.79	163.13	125.73	24.26	0.62	3.64	3.33	1.50
SX08	H	H	H	H	205.3	222.72	84.63	2.92	3.18	3.18	2.08

Appendix 3: Radiographic Callus Measurements

Animal	Callus Index			Coronal Width (pixel units)	Sagittal Width (pixel units)
	2 weeks	4 weeks	6 weeks		
CX01	1.31	1.57	1.57	4.405	4.67
CX02	1.00	1.14	1.48	3.883	3.6
CX03	1.00	1.52	1.65	5.385	5.73
CX04	1.05	1.40	1.61	5.803	7.73
CX05	1.00	1.41	1.60	5.803	5.6
CX06	1.00	1.36	1.56	5.064	5.17
CX07	1.00	1.38	1.60	4.8	4.8
CX08	1.00	1.38	1.57	5.192	4.03
SX01	1.46	2.04	1.33	5.636	5.87
SX02	1.00	1.27	1.36	4.418	5.47
SX03	1.06	1.24	1.11	3.883	3.2
SX04	1.19	1.59	1.13	4.754	4.83
SX07	1.00	1.15	1.13	3.406	3.6
SX08	1.36	1.73	1.60	4.817	4.73

Appendix 4: Radiographic Scoring of Osteotomy Line

	Author		Independent Assessor	
Occasion	First	Second	First	Second
Animal				
C01	2	2	2	2
C03	1	1	1	1
C04	2	2	2	2
C05	1	1	1	1
C06	1	1	1	2
C07	2	2	2	2
C08	2	2	1	2
C09	2	2	2	2
C10	1	1	1	1
CX01	2	2	2	2
CX02	2	2	2	2
CX03	1	1	2	1
CX04	1	1	1	1
CX05	1	1	1	2
CX06	1	2	1	1
CX07	1	1	0	1
CX08	2	2	2	2
S02	1	1	1	1
S03	0	1	0	1
S04	0	0	0	0
S05	1	1	0	0
S06	1	1	1	1
S07	0	0	0	0
S08	1	1	1	1
S09	0	0	0	0
S10	0	0	0	0
SX01	1	1	1	1
SX02	1	1	1	1
SX03	2	2	2	1
SX04	2	2	1	2
SX07	2	2	2	1
SX08	2	1	1	1

Appendix 5: Animal Weights

Animal	Weight at Fracture (g)	Weight at Sacrifice (g)
C01	468	475
C02	611	617
C03	475	467
C04	477	480
C05	450	476
C06	479	516
C07	456	483
C08	475	492
C09	527	529
C10	421	439
CX01	438	463
CX02	454	450
CX03	456	477
CX04	601	603
CX05	468	462
CX06	483	481
CX07	514	533
CX08	492	481
S01	524	516
S02	522	510
S03	510	509
S04	500	494
S05	525	519
S06	536	552
S07	482	495
S08	532	540
S09	527	519
S10	472	465
SX01	416	410
SX02	519	507
SX03	441	448
SX04	504	508
SX05	494	501
SX06	577	559
SX07	576	545
SX08	475	489